Simulation Studies of Protein-Induced Bilayer Deformations, and Lipid-Induced Protein Tilting, on a Mesoscopic Model for Lipid Bilayers with Embedded Proteins

Maddalena Venturoli,*† Berend Smit,* and Maria Maddalena Sperotto‡
*Department of Chemical Engineering, University of Amsterdam, Amsterdam, The Netherlands; †Department of Chemistry, University College, London, United Kingdom; and ‡Biocentrum, The Technical University of Denmark, Kgs. Lyngby, Denmark

ABSTRACT Biological membranes are complex and highly cooperative structures. To relate biomembrane structure to their biological function it is often necessary to consider simpler systems. Lipid bilayers composed of one or two lipid species, and with embedded proteins, provide a model system for biological membranes. Here we present a mesoscopic model for lipid bilayers with embedded proteins, which we have studied with the help of the dissipative particle dynamics simulation technique. Because hydrophobic matching is believed to be one of the main physical mechanisms regulating lipid-protein interactions in membranes, we considered proteins of different hydrophobic length (as well as different sizes). We studied the cooperative behavior of the lipid-protein system at mesoscopic time- and lengthscales. In particular, we correlated in a systematic way the protein-induced bilayer perturbation, and the lipid-induced protein tilt, with the hydrophobic mismatch (positive and negative) between the protein hydrophobic length and the pure lipid bilayer hydrophobic thickness. The protein-induced bilayer perturbation was quantified in terms of a coherence length, ξ_P, of the lipid bilayer hydrophobic thickness profile around the protein. The dependence on temperature of ξ_P, and the protein tilt-angle, were studied above the main-transition temperature of the pure system, i.e., in the fluid phase. We found that ξ_P depends on mismatch, i.e., the higher the mismatch is, the longer ξ_P becomes, at least for positive values of mismatch; a dependence on the protein size appears as well. In the case of large model proteins experiencing extreme mismatch conditions, in the region next to the so-called *lipid annulus*, there appears an *undershooting* (or *overshooting*) region where the bilayer hydrophobic thickness is locally lower (or higher) than in the unperturbed bilayer, depending on whether the protein hydrophobic length is longer (or shorter) than the pure lipid bilayer hydrophobic thickness. Proteins may tilt when embedded in a too-thin bilayer. Our simulation data suggest that, when the embedded protein has a small size, the main mechanism to compensate for a large hydrophobic mismatch is the tilt, whereas large proteins react to negative mismatch by causing an increase of the hydrophobic thickness of the nearby bilayer. Furthermore, for the case of small, peptidelike proteins, we found the same type of functional dependence of the protein tilt-angle on mismatch, as was recently detected by fluorescence spectroscopy measurements.

INTRODUCTION

Biological membranes are complex, organized, dynamic, and highly cooperative structures whose physical properties are important regulators of vital biological functions ranging from cytosis and nerve processes, to transport of energy and matter (Sackmann, 1995). To relate the structure and dynamics of biomembranes to their biological function (the ultimate goal of biomembrane science), it is often necessary to consider simpler systems. Lipid bilayers composed of one or two lipid species with embedded proteins, or natural or artificial peptides, provide a model system for biological membranes. Understanding the physics of such simplified soft-condensed matter systems can yield insight into biological membrane functions. Therefore these systems are extensively investigated, both experimentally and theoretically.

The hydrophobic matching between the lipid bilayer hydrophobic thickness and the hydrophobic length of integral membrane proteins has been proposed as one of the main physical mechanisms that regulate the lipid-protein interaction in biomembranes (Mouritsen and Blom, 1984; Sackmann, 1984; Mouritsen and Sperotto, 1993; Gil et al., 1998; Killian, 1998; Dumas et al., 1999). The energy cost of exposing polar moieties, from either hydrocarbon chains or protein residues, is so high that the hydrophobic part of the lipid bilayer should match the hydrophobic domain of membrane proteins. The results from a number of investigations have indeed pointed out the relevance of the hydrophobic matching in relation to the lipid-protein interactions, hence to membrane organization and biological function. It is now known that hydrophobic matching is used in cell membrane organization: the membranes of the Golgi have different thicknesses; along their secretory pathway, proteins that pass through the Golgi undergo changes of their hydrophobic length to match the membrane hydrophobic thickness of the Golgi (Munro, 1995,1998; Bretscher and Munro, 1993; Pelham and Munro, 1993). Hydrophobic matching seems also to play a role in sequestering proteins with long transmembrane regions (McIntosh et al., 2003) into sphingolipids-cholesterol biomembrane domains denoted *rafts* (Simons and Ikonen, 1997; Binder et al., 2003).

Submitted August 2, 2004, and accepted for publication October 22, 2004.

Address reprint requests to Maria Maddalena Sperotto, E-mail: maria@cbs.dtu.dk.

0006-3495/05/03/1778/21 $2.00

doi: 10.1529/biophysj.104.050849

The biological importance of rafts, and their involvement in Alzheimer's and prion diseases, is nowadays an intensively investigated subject (Fantini et al., 2002).

Biological membranes have at their disposal a number of ways to compensate for hydrophobic mismatch (de Planque and Killian, 2003), which may be used individually or simultaneously. These ways may imply changes of the membrane structure and dynamics on a microscopic, as well as on a macroscopic scale, and therefore can affect the membrane biological function (Montecucco et al., 1982; Johansson et al., 1981; In't Veld et al., 1991; Lee, 1998). To adjust to hydrophobic mismatch a membrane protein may cause a change of the lipid bilayer hydrophobic thickness in its vicinity. Experimental studies on reconstituted systems show that the range of the perturbation induced by proteins on the membrane thickness varies considerably from system to system (Jost et al., 1973; Hesketh et al., 1976; Jost and Hayes Griffith, 1980; Rehorek et al., 1985, Piknová et al., 1993; Harroun et al., 1999; Bryl and Yoshihara, 2001). A lipid sorting at the lipid-protein interface may also occur, where the protein prefers, on a statistical basis, to be associated with the type of lipid that best matches its hydrophobic surface (Dumas et al., 1997; Lehtonen and Kinnunen, 1997; Fahsel et al., 2002; Fernandes et al., 2003). Another way that a protein may have to adapt to a too-thin lipid bilayer is to tilt (Glaubitz et al., 2000; Killian, 1998; Sharpe et al., 2002; van der Wel et al., 2002; Koehorst et al., 2004; Strandberg et al., 2004). In addition to the protein as a whole, the individual helices of which a protein might be composed may also experience a tilt; and there is indeed some experimental evidence that the latter phenomenon may occur in channel proteins (Lee, 2003), and that a change in tilt-angle of the individual helices could be the cause of a change in protein activity. Long and single-spanning membrane proteins might also bend to adapt to a too-thin bilayer. Spectroscopic measurements on phospholipid bilayers, with embedded poly(leucine-alanine) α-helices, suggest that the conformation of long peptides deviates from a straight helical end-to-end conformation (Harzer and Bechinger, 2000; Strandberg et al., 2004). A protein may also undergo structural changes to adapt to a mismatched lipid bilayer. Spectroscopy measurements indicate that, indeed, long hydrophobic polyleucine peptides might distort in the C- and N-terminus to reduce their hydrophobic length and thus match the thickness of the lipid bilayer in the gel-phase (Liu et al., 2002). Lipid-mediated protein aggregation could also occur to reduce the stress caused by hydrophobic mismatch (Mall et al., 2001; Fernandes et al., 2003; Harroun et al., 1999). Domains (Binder et al., 2003) may thus form whose functional properties differ from those of the *bulk*, i.e., the unperturbed bilayer (Tocanne, 1992; Tocanne et al., 1994; Thomson et al., 1995). When the degree of mismatch is too high to be counterbalanced by the adaptations just described, the proteins might partition between an in-plane and a transmembrane orientation, or even avoid incorporation in the membrane (Harzer and Bechinger, 2000; de Planque et al., 2001; Ridder et al., 2002). The phenomena just mentioned refer to local microscopic changes related to mismatch adjustment. Perturbations of the membrane on the macroscopic scale may also occur; these can range from in-plane protein segregation and crystallization, and gel-fluid phase separation (Mouritsen, 1998; Gil et al., 1998; Dumas et al., 1997; Morein et al., 2002; Fahsel et al., 2002), to changes of the three-dimensional structure of the membrane. The formation of nonbilayer phases upon protein incorporation in lipid bilayers is an example of the latter type of phenomena (Killian, 1992; Epand, 1998).

In an effort to elucidate the effects caused at the molecular level by the lipid-protein hydrophobic mismatch, and even their possible implications for the formation of biologically relevant domainlike structures such as rafts, a number of theoretical studies have been done with the help of different types of theoretical models (Sperotto and Mouritsen, 1991; Fattal and Ben-Shaul, 1993; Mouritsen et al., 1996; Gil and Ipsen, 1997; Belohorcová et al., 1997, 2000; Sintes and Bäumgartner, 1998; Dan and Safran, 1998; Nielsen et al., 1998; May, 2000; Duque et al., 2002; Petrache et al., 2000b, 2002; Jensen et al., 2001, 2002; Shen et al., 1997; Bohinc et al., 2003; Jensen and Mouritsen, 2004). One of the quantities that has drawn considerable attention in recent years is the extension of the domain size, which is determined by the coherence length of the spatial fluctuations occurring in the system. Such fluctuations, which depend on the thermodynamic state of the system, can be induced, as well as harvested, by proteins. In the past, computer simulations have been made on a lattice model to measure the extent of the perturbation induced by a protein on the surrounding lipid bilayer (Sperotto and Mouritsen, 1991). The results from these simulations indicated that the extension of the perturbation depends on factors such as the degree of hydrophobic mismatch, the size of the protein (i.e., the curvature of the protein hydrophobic surface in contact with the lipid hydrocarbon chains), and on the temperature of the investigated system. Also, it was found that, away from the protein, the perturbation decays in an exponential manner, and can therefore by characterized by a decay length, ξ_P. The value ξ_P is a measure of the size of small-scale inhomogeneities (i.e., domains) experienced by proteins when embedded in the lipid bilayer. In a sense, ξ_P is also a measure of the extension of the range over which the lipid-mediated interaction between proteins may operate. Results from model studies of a phenomenological interfacial model for proteinlike objects in a bilayerlike system suggest that, under well-defined thermodynamic conditions, the protein-induced perturbation may propagate without decay over a number of lipid shells around the protein (the number of lipid shells being dependent, among other factors, on the size of the protein), may extend over long ranges, and might eventually establish a thermodynamic phase (Gil and Ipsen, 1997; Gil et al., 1998). The phase of the multilayered

region that the protein prefers to be surrounded with is thus said to *wet* the protein (Gil and Ipsen, 1997; Gil et al., 1998). The disadvantage of using models such as the lattice models (Sperotto and Mouritsen, 1991) or the phenomenological models (Gil and Ipsen, 1997; Gil et al., 1998; Dan and Safran, 1998; Nielsen et al., 1998) is that these models do not allow for tilting of the model proteins as a whole. Therefore, with the help of these models, one cannot make predictions about the physical hydrophobic-mismatch condition that induce a protein to tilt in the lipid bilayer, other than, at the same time, by inducing a bilayer deformation in the vicinity of the protein. With the help of a microscopic model, Duque et al., (2002) have indeed studied how hydrophobic mismatch affects the way in which the inclination of transmembrane helices changes as a function of their hydrophobic length. Their self-consistent calculations predicted that peptides, whose hydrophobic length is less than that of the hydrophobic bilayer thickness, insert perpendicular to the bilayer—whereas peptides with a longer hydrophobic length than the bilayer hydrophobic thickness insert into the bilayer in a tilted manner, and with an angle with the bilayer-normal that increases with increasing mismatch.

The types of models described above are relatively crude, in the sense that either they cannot be used to investigate the physical conditions that cause protein tilting, or they do not take into full account the three-dimensional molecular structure of the bilayer. Simulations on more realistic models, such as all-atom models for lipid bilayers with embedded proteins, have confirmed that, at least within a time of the order of the nanoseconds, a mismatched protein can induce a deformation of the lipid bilayer structure (Chiu et al., 1999; Petrache et al., 2000b, 2002; Jensen et al., 2001), and that the deformation is of the exponential type (Jensen and Mouritsen, 2004). The same type of studies have also shown that tilting may also occur for membrane peptides (Belohorcová et al., 1997; Shen et al., 1997); however, to reduce a possible hydrophobic mismatch, synthetic peptides might instead prefer to deform the lipid bilayer, rather than undergo tilting (Petrache et al., 2002). Incidentally, the results from these studies indicated that the helical-peptides experience a slight bend in the middle of the helix.

Regardless of the huge body of experimental and theoretical studies on lipid bilayers with embedded proteins, issues like the range of the protein-induced lipid bilayer perturbation, its dependence on protein size, and the simultaneous occurrence of protein tilting (or even bending) to adjust for hydrophobic mismatch, are still a matter of debate. In this article we want to focus on these issues, which we investigate by means of a mesoscopic model for lipid bilayers with embedded proteins and a relatively new simulation method. Before introducing the model and the method, we would like to sketch the historical background that brought scientists to the development of mesoscopic models to study physical phenomena in biomembranes.

Because of the many degrees of freedom involved, the processes that take place even in model biomembranes occur over a wide range of time- and lengthscales (König and Sackmann, 1996). To model membranes, it is thus necessary to decide, a priori, the level of description of the system (i.e., to deliberately neglect those details unimportant to the process one wants to investigate). Often, this necessity follows the fact that some theoretical methods are limited in their applicability by the long computational times needed to calculate statistical quantities. The drawbacks of those otherwise relatively noncomputationally-time-demanding phenomenological, lattice, or interfacial models have outlined the necessity of more realistic models to investigate the effect of proteins on the bilayer structure and dynamics. Molecular dynamics (MD) simulation methods on all-atom models have been used to study the self-assembly of phospholipids into bilayers (Marrink et al., 2001) as well as the structure, dynamics, and interactions of individual membrane peptides or proteins with the lipid bilayer (Shen et al., 1997; Belohorcová et al., 1997, 2000; Jensen et al., 2001; Jensen and Mouritsen, 2004). MD simulations can provide detailed information about the phenomena that occur in biomembrane systems, although at the nanoscopic level and on a nanosecond timescale. Many membrane processes happen at mesoscopic length- and timescales, however—that is, above 1–1000 nm, and 1–1000 ns, respectively—and involve the collective nature of the system. This is the case for phenomena related to the gel-fluid phase transition and phase separation, the formation of domains on the mesoscopic scale, or the transition from a bilayer to a nonbilayer phase. Even though the speed of numerical computation is increasing very rapidly, it will be some time before it will be possible, by MD on realistic all-atom models, to predict the cooperative behavior of biosystems at mesoscopic timescales. Numerical studies of these phenomena require a considerable simplification of the model. These simplifications can be made by using a system of particles, or *beads*, in which each particle represents a complex molecular component of the system whose details are not important to the process under investigation. These models with simplified interactions between the beads are called coarse-grain (CG) or mesoscopic models. In recent years, CG models have been developed to study the phase equilibria of biomembrane-like systems at the mesoscopic level, and both MD and Monte Carlo (MC) simulation methods were used on such models (Goetz and Lipowsky, 1998). With the minimal modeling approach it was possible to simulate the self-assembly of phospholipids into various phases, both in the absence and presence of such biologically relevant molecules as anesthetics and alkanes (Shelley et al., 2001a,b). It was also possible to study the lipid-mediated range of attraction between two proteins embedded in a lipid bilayer (Sintes and Bäumgartner, 1998).

Despite the advantages that arise by minimal modeling in connection with simulation methods like MD and MC, the possibility to study processes that involve the collective

behavior of the system is still limited. To try to overcome this limitation, the use of a faster simulation technique, i.e., dissipative particle dynamics (DPD), on CG models has thus been considered. The DPD-on-CG-model approach can be seen as a middle course between the approach based on pseudo-three-dimensional models (such as lattice and interfacial models) and the one based on all-atom models. The DPD method was originally developed to simulate complex fluids, such as surfactant and polymer melts, at the mesoscopic level. It was then adopted to study mesoscopic models for pure lipid bilayer systems (Venturoli and Smit, 1999), as well as lipid bilayers containing impurities such as alcohols (Kranenburg and Smit, 2004; Kranenburg et al., 2004b). The results from the simulation studies demonstrated that with the DPD-CG approach one was able to reproduce the structural and thermodynamic properties resulting from cooperative behavior of the lipid bilayer system (Kranenburg et al., 2003a,b).

We have adopted the DPD simulation method to study the behavior of a mesoscopic model for lipid bilayers with embedded proteins. The model was derived from the mesoscopic model for pure lipid bilayers (Venturoli and Smit, 1999) and was extended to account for the presence of proteins. We studied systems at low protein/lipid ratios.

The aim of the work presented in this article was to understand whether, and to what extent due to hydrophobic mismatch, and via the cooperative nature of the system, a protein may prefer to tilt (with respect to the normal of the bilayer plane), rather than to induce a bilayer deformation without (or even with) tilting. Therefore we have attempted to make a systematic correlation of the protein-induced perturbation and lipid-induced protein tilting with hydrophobic mismatch.

The article is structured as follows. First we describe the mesoscopic model for lipid bilayers with embedded proteins, and present the DPD simulation method. We then present the model parameters, the statistical ensemble used for the simulations, and the methods of calculation of statistical quantities. In Results and Discussion, data for both pure lipid bilayers and those with embedded proteins are shown and discussed. Whenever possible, we have validated the model by comparing the results obtained from our model study with existing theoretical and experimental data. The results from the simulation studies and the model predictions are summarized in Conclusion and Future Perspectives, together with possible future applications of the DPD-on-CG-model approach.

MODEL AND SIMULATION METHOD

Mesoscopic model

Within the mesoscopic approach, each molecule of the system (or groups of molecules) is coarse-grained by a set of beads. In the specific case of the lipid-protein system, we considered three types of beads: a waterlike bead, labeled w; a hydrophilic bead, labeled h, which models a part of the headgroup of either the lipid or the protein; and a hydrophobic bead, labeled either t_L or t_P, depending on whether it refers to a portion of the lipid hydrocarbon chain or a portion of the hydrophobic region of the protein, respectively. Each model-lipid is built by one or more headgroup-like h-beads connected to two tails of equal length. Each of these tails is formed by connecting with springs a chosen number of t_L-beads, depending on the type of lipids one wants to model. Fig. 1 *a* shows a schematic representation of a model-lipid. A w-water-bead represents three water molecules, and a t-bead represents three CH_2 groups (or one CH_2 plus one CH_3 group) of the lipid hydrocarbon chain (Kranenburg et al., 2004a). The systems that we have simulated are made of model-lipid chains having three headgroup beads and five beads in each chain; this corresponds to the case of an acyl chain with 14 carbon atoms, namely to a model for a dimyristoylphosphatidylcholine phospholipid, as illustrated in Fig. 2.

Within the model formulation, a protein is considered as a rodlike object, with no appreciable internal flexibility, and characterized by a hydrophobic length. The model for the transmembrane protein is built first by connecting n_{t_P} hydrophobic-like beads into a chain, to the ends of which are attached n_h headgroup-like beads; these are then linked together into a bundle of N_P of these amphiphatic bead-chains. In each model protein, all the N_P chains are linked to the neighboring ones by springs, to form a relatively rigid body. We have considered three typical model-protein sizes, two of them referring to a skinny peptidelike molecule, consisting of $N_P = 4$ and 7 chains, respectively, and the third type to a fat protein, consisting of $N_P = 43$ chains. The bundle of $N_P = 7$ chains is formed by a central chain surrounded by a single layer of six other chains. The $N_P = 43$ bundle is made of three layers arranged concentrically around a central chain, with each containing 6, 12, and 24 amphiphatic chains, respectively. The number of beads at each hydrophilic end of the bead-chains forming the protein is set equal to 3. Each protein hydrophobic bead, t_P, corresponds to a section of an α- or β-helical membrane protein. The distance spanned by a bead corresponds approximately to that spanned by a helix turn. Regarding the chosen protein

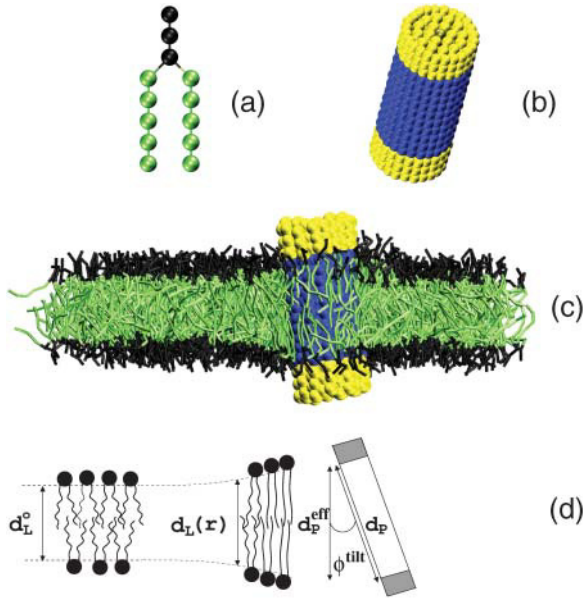

FIGURE 1 Schematic representation of a model lipid (*a*), and a model protein ($N_P = 43$ and $\tilde{d}_p = 41$Å) (*b*). A typical configuration of the assembled bilayer with a model protein embedded (as results from the simulations) is shown in the snapshot (*c*). The drawing in *d* shows the part of the system to which the following quantities refer: the pure lipid bilayer hydrophobic thickness, d_L^o; the perturbed lipid bilayer hydrophobic thickness, $d_L(r)$; the protein hydrophobic length, d_P; the tilted-protein hydrophobic length, d_P^{eff}; and the tilt-angle, ϕ^{tilt}.

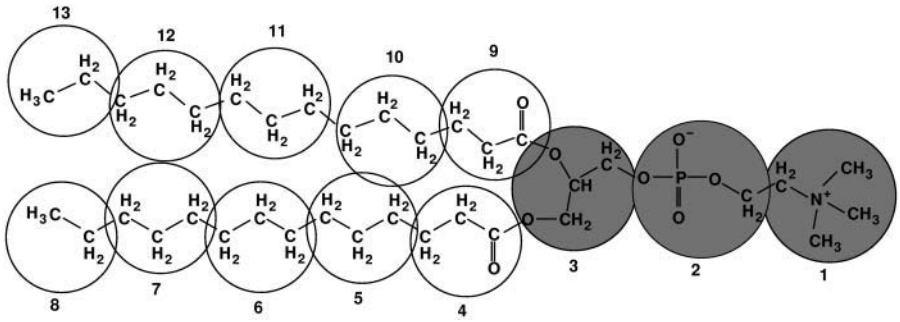

FIGURE 2 The atomistic representation of DMPC and its corresponding coarse-grained model. Hydrophilic head-beads are indicated in shading and hydrophobic tail-beads in open representation.

sizes, $N_P = 4$, 7, and 43, and their relation to those of actual proteins, the hydrophobic section of single-spanning membrane proteins like glycophorin (MacKenzie et al., 1997) and the M13 major coat protein from phage (Stopar et al., 2003, Bechinger, 1997) or α-helical synthetic peptides (Morein et al., 2002) may be modeled by a skinny $N_P = 4$ type. β-helix proteins like gramicidin A (Killian, 1992) may be modeled by a $N_P = 7$ type. The fat protein may be a model for larger proteins consisting of transmembrane α-helical peptides that associate in bundles, or β-barrel proteins (von Heijne and Manoil, 1990). Specific examples could be bacteriorhodopsin (Henderson and Unwin, 1975), lactose permease (Foster et al., 1983), the photosynthetic reaction center (Deisenhofer et al., 1985), cytochrome *c* oxidase (Iwata et al., 1995), or aquaglyceroporin (Fu et al., 2000). Because we were interested in mismatch-dependent effects, we have chosen protein hydrophobic sections composed of chains with the following number of hydrophobic beads: $n_{t_P} = 2$, 4, 6, 8, 10, and 12. Fig. 1 *b* shows a cartoon of a model protein of size $N_P = 43$, and Fig. 1 *c* shows a snapshot of a typical configuration of the assembled bilayer that has an embedded protein; these simulation results will be discussed later on.

Dissipative particle dynamics

We studied the mesoscopic model with the help of the dissipative particle dynamics (DPD) simulation method (Hoogerbrugge and Koelman, 1992; Warren, 1998; Jury et al., 1999). The DPD method was originally based on the idea of simulating the fluid hydrodynamics of systems composed of particles, or *beads*, in analogy with the way the Navier-Stokes equations reproduce the motion of a real fluid. Each bead, which represents the center of mass of a small droplet of the fluid, moves according to Newton's equation of motion, and interacts according to simplified force laws. The beads interact with each other via conservative, random, and dissipative forces of the pairwise-additive type. The total force, $\mathbf{f}_i$, acting on bead *i*, is thus expressed as a sum over all other beads, *j*, which are within a certain cutoff radius R_c from bead *i*,

$$\mathbf{f}_i = \sum_{j \neq i} (\mathbf{F}^C_{ij} + \mathbf{F}^D_{ij} + \mathbf{F}^R_{ij}). \tag{1}$$

The first term in Eq. 1 refers to a force of conservative type. This comprises two contributions, one related to interactions between beads not bound together, and the other related to interactions between beads that are linked together. The former contribution is chosen in such a way to model a soft-repulsive potential,

$$\mathbf{F}^C_{ij} = \begin{cases} a_{ij}(1 - r_{ij}/R_c)\hat{\mathbf{r}}_{ij} & (r_{ij} < R_c) \\ 0 & (r_{ij} \geq R_c) \end{cases}, \tag{2}$$

where the coefficients $a_{ij} > 0$ represent the maximum repulsion strength, $\mathbf{r}_{ij} = \mathbf{r}_i - \mathbf{r}_j$ is the distance between bead-particles *i* and *j*, and R_c is the cutoff radius, which gives the extent of the interaction range. The conservative force can have also an elastic contribution, which derives from the harmonic force used to tie two consecutive beads in the chains of either the lipid or the protein. This contribution is expressed as

$$\mathbf{F}_{spring} = -K_r(r_{ij} - r_{eq})\hat{\mathbf{r}}_{ij}, \tag{3}$$

where K_r is the elastic constant, and r_{eq} is the equilibrium value of r_{ij}. To control the chain flexibility, an extra bond-bending force between consecutive bonds is added,

$$\mathbf{F}_\theta = -\nabla U_\theta, \tag{4}$$

$$U_\theta = \frac{1}{2} K_\theta (\theta - \theta_o)^2, \tag{5}$$

where K_θ is the bending constant, θ is the angle between two consecutive bonds, and θ_o is the equilibrium angle. The other two forces in Eq. 1 are a drag force ($\mathbf{F}^D$) and a random force ($\mathbf{F}^R$), which are expressed as

$$\begin{aligned} \mathbf{F}^D_{ij} &= -\eta w^D(r_{ij})(\hat{\mathbf{r}}_{ij} \cdot \mathbf{v}_{ij})\hat{\mathbf{r}}_{ij} \\ \mathbf{F}^R_{ij} &= \sigma w^R(r_{ij})\zeta_{ij}\hat{\mathbf{r}}_{ij}, \end{aligned} \tag{6}$$

where $\mathbf{v}_{ij} = \mathbf{v}_i - \mathbf{v}_j$ is the velocity difference between particles *i* and *j*, η is the friction coefficient, and σ is the noise amplitude. The quantity ζ_{ij} is a random number, which is chosen from a uniform random distribution, and in an independent manner for each pair of particles. The chosen functional dependence on $\mathbf{r}_{ij}$ of the conservative force, $\mathbf{F}^C$, permits us to use larger integration time-steps than are usually allowed by the MD simulation technique (which has to do with computationally demanding forces of the Lennard-Jones hard-core type). Also, the combined effect of the two forces, the dissipative and the random, acts as a thermostat—which conserves the (angular) momentum and thus provides the correct hydrodynamics to the system, at least for sufficiently long timescales and large system sizes.

Español and Warren (1995) have shown that the equilibrium distribution of the system is the Gibbs-Boltzmann distribution, if the weight functions and coefficients of the drag and random forces satisfy

$$w^D(r) = [w^R(r)]^2, \tag{7}$$

$$\sigma^2 = 2\eta k_B T, \tag{8}$$

where k_B is the Boltzmann constant and T is the temperature. Furthermore, all the forces assume the same functional dependence on the interparticle distance $\mathbf{r}_{ij}$ (as the conservative force $\mathbf{F}^C_{ij}$ does) if the weight function $w^R(r)$ is of the type

$$w^R(r) = \begin{cases} (1 - r/R_c) & (r < R_c) \\ 0 & (r \geq R_c) \end{cases}. \tag{9}$$

Model parameters

The repulsion parameter (see Eq. 2) related to the interaction between the water beads, a_{ww}, was derived by fitting the calculated value of the compressibility of water, at room temperature, to the experimental one (Groot and Warren, 1997). In principle, this fitting procedure may be applied

at any temperature, and may thus result in temperature-dependent a_{ij} parameters. To deal with temperature-dependent parameters would make the interpretation of the simulation data very difficult. Therefore, we make an approximation in which we assume that the parameters a_{ij} are not temperature-dependent. These parameters have been chosen so as to reproduce the structural and thermodynamic behavior of the pure system, i.e., of a pure DMPC bilayer. Because a direct mapping between the atomic level information and the model parameters is not always possible, it is worth mentioning that these are effective parameters and reflect this limitation. Therefore, it will not always be possible to make a direct comparison between the properties of the model system and the properties of the reconstituted system.

The values of the parameters referring to the lipid-lipid and lipid-water interaction have been chosen equal to those used for the pure lipid bilayer model (Kranenburg et al., 2003a). To model the amphiphilic nature of the lipids, the repulsion parameters a_{ij} (Eq. 2) between two beads (whether hydrophilic or hydrophobic) were chosen to be smaller than the repulsion parameters between two beads of which one is hydrophilic and the other hydrophobic. The numerical values of the interaction parameters between different bead types are given in Table 1.

Regarding the protein-protein interactions, the values of parameters related to the repulsive interactions between the beads forming the hydrophilic part of the protein, as well as those between the protein-hydrophobic beads, have been chosen equal to the ones pertaining to the interaction between the hydrophilic and the hydrophobic beads of the lipid, respectively. Their values are therefore $a_{hh} = 35$ and $a_{t_P t_P} = a_{t_L t_L} = 25$. For the parameter related to the interaction between the protein hydrophobic beads and the water, we have chosen the value $a_{wt_P} = 120$, which ensures that the hydrophobic section of the protein is sufficiently shielded from the water environment.

Concerning the elastic contribution to the interaction energy (see Eq. 3), at an overall bead density of 3 (Groot and Warren, 1997), the resulting equilibrium distance is equal to $r_{eq} = 0.7$. To determine the spring constant, K_r, for the lipid chain, we required that 98% of the bond-distance distribution be within one R_c. A value of $K_r = 100$ was found to satisfy this requirement.

The values of the parameters related to the bond-bending force (Eq. 4) for the model lipids were derived from MD simulations on an all-atom model for a DMPC lipid bilayer (Kranenburg et al., 2004a). The resulting values for the bending constant and the equilibrium angle in the lipid tails are $K_\theta = 6$ and $\theta_o = 180°$, respectively. For the bond-bending potential between the head-bead connected to the lipid tails and the first beads in the tails (beads 3, 4, and 9 in Fig. 2), values of $K_\theta = 3$ and $\theta_o = 90°$ were found to reproduce the correct configurational distribution, and structure, of the all-atom model for a DMPC lipid molecule.

Compared to the lipid hydrocarbon chains, the hydrophobic part of membrane proteins can be considered fairly rigid; therefore the value of the bending constant in the protein chains was set equal to $K_\theta = 100$, i.e., an order-of-magnitude larger than that used for the lipid chains. The equilibrium spring-distance and spring constant between the beads in the protein chains were chosen equal to the values used for the lipid chains, i.e., $r_{eq} = 0.7$ and $K_r = 100$, respectively.

Length-, time-, and temperature-scales

Usually, within the DPD approach, one makes use of reduced units for the mass, length, and energy (Groot and Warren, 1997; Groot and Rabone, 2001). The DPD unit of length is the cutoff radius, R_c, the unit of mass is the mass, m, of a bead (where all the beads in the system have equal mass), and the unit of energy is k_BT. Therefore the temperature is expressed in reduced units as well. Before presenting our results, we would like to spend a few words to give an estimate of the typical time- and lengthscales (expressed in terms of physical units) involved when one uses the DPD simulation method.

TABLE 1 Repulsion parameters a_{ij} (Eq. 2) used for the interactions between the different bead-types

a_{ij}	w	h	t_L	t_P
w	25	15	80	120
h	15	35	80	80
t_L	80	80	25	25
t_P	120	80	25	25

For the lengthscale, one can say that the level of coarse-graining (i.e., the number, N_m, of atoms, or molecules, represented by a DPD bead), is the renormalization factor for the mapping of the reduced units of length onto physical units. To estimate the value of the cutoff radius, R_c, one can reason as follows (Groot and Rabone 2001): If a DPD bead corresponds to N_m water molecules, then a cube of volume R_c^3 represents ρN_m water molecules, where ρ is the density, i.e., the number of DPD beads per cubic R_c. Assuming that a water molecule has approximately a volume of 30 Å^3, one obtains

$$R_c = 3.107(\rho N_m)^{1/3}[\text{Å}]. \quad (10)$$

If a bead density equal to $\rho = 3$ (Groot and Warren, 1997) is chosen, the cutoff radius is then equal to

$$R_c = 4.48(N_m)^{1/3}[\text{Å}]. \quad (11)$$

As previously detailed in Mesoscopic Model, the results discussed below refer to a coarse-graining with $N_m = 3$. The choice of $N_m = 3$ results in a DPD bead having the volume of three water molecules, i.e., 90 Å^3. Therefore, from Eq. 11 one obtains $R_c = 6.46$ Å. This value may then be used to convert the reduced units of length into Ångstrøms.

In the literature, different mapping criteria have been adopted to derive the physical unit of time, τ. All these criteria were based on the mapping of the experimental value of the diffusion constants of one of the components of the system onto the value obtained from the simulations. For example, Groot and Rabone (2001) considered the self-diffusion constant of water, whereas Groot (2000) used the diffusion constant of a surfactant micelle. In both cases, a value of the integration timestep, $\Delta t = 0.06\tau$, was used, which gave $\Delta t \approx 5$ ps and $\Delta t \approx 25$ ps, respectively. Both of these values show that DPD simulations allow for a timestep that is at least three orders-of-magnitude longer than that used in atomistic MD simulations, which is typically of the order of a few femtoseconds.

To give an estimate of the values of the reduced temperatures in terms of physical temperatures, we have mapped the reduced temperatures, T^*, onto physical temperatures, T, according to the linear relation

$$T = aT^* + b. \quad (12)$$

The values of the coefficients a and b were found by solving the system of linear equations obtained by substituting in Eq. 12 the reduced and physical values of the main- and pre-transition temperatures, 24°C and 13.5°C (Koynova and Caffrey, 1998), respectively, for a pure DMPC phospholipid bilayer. The resulting values are $a = 133$°C and $b = -33$°C.

Statistical ensemble and surface tension

It has been suggested (Jähnig, 1996) that unconstrained, self-assembled bilayers are at their free-energy minimum, characterized by having a zero value of the surface tension. Nevertheless, it is still a matter of debate which value of the surface tension should be used in molecular simulations. For both self-assembled and preassembled membranes, a fixed number of lipid molecules and a fixed area combined with periodic boundary conditions are generally used in MD simulations. Periodic boundary conditions minimize the effects due to the finite size of the bilayer, but the fixed size of the simulation box imposes a constraint on the bilayer, which might also result in a finite surface tension. Although the constraint on the fixed area can be released by performing simulations at constant pressure or constant surface tension (Chiu et al., 1995, Zhang et al., 1995), there is still the question of which value of the surface tension should be used to reproduce the area per lipid of a simulated lipid bilayer. In their molecular dynamics simulations, Feller and Pastor (1996, 1999) observed that a tensionless state did not

reproduce the value of the area per lipid derived from experiments. They argued that this is because the typical undulations and out-of-plane fluctuations of a macroscopic membrane cannot develop in a patch of a membrane, whose size is similar to that considered during MD simulations. They concluded that a positive surface tension (stretching) must be imposed on the system to compensate for the suppressed undulations, and to be able to reproduce the value of the area per lipid calculated from experiments. However, more recently, Marrink and Mark (2001) investigated the system size-dependence of the surface tension in large membrane patches ranging from 200 to 1800 lipids, simulated for times up to 40 ns. These authors found that simulations at zero surface tension correctly reproduce the experimental surface areas for an unstressed membrane. Goetz et al. (1998) suggested performing simulations for the exact area at which the interfacial tension is 0, and to determine this area iteratively. We have adopted a different approach, in which we mimic the experimental condition by simulating a system in which we impose a value of the surface tension. To be able to impose a given value of the surface tension on the model system, we have adopted a hybrid scheme based on both the DPD and the Monte Carlo (MC) simulation methods. The DPD method was used to evolve the positions of the beads; the Newton's equations of motion were integrated by adopting a modified version of the velocity Verlet algorithm (Groot and Warren, 1997). The MC method was used to impose a given surface tension on the bilayer. This was done by changing the bilayer projected area on the plane perpendicular to the bilayer normal, A, by an amount, ΔA, and, at the same time, by changing the height of the simulation box to ensure that the total volume of the system remains constant (Venturoli and Smit, 1999), and therefore no work is done against the external pressure. The MC acceptance probability, P_{acc}, was expressed as

$$P_{\mathrm{acc}} = \frac{\exp\{-\beta[U' - \gamma(A + \Delta A)]\}}{\exp\{-\beta[U - \gamma A]\}}, \tag{13}$$

where U and U' define the energies before and after the change of the box sizes, respectively, and where $\beta = 1/k_{\mathrm{B}}T$. To obtain the tensionless state of the bilayer, γ was set to zero in Eq. 13.

Before collecting the data used to estimate the statistical quantities of interest, we have first equilibrated each bilayer system for 20,000 DPD-MC cycles. In each cycle it was chosen, with a probability of 70%, whether to perform a number of DPD steps, or to attempt to change the box aspect-ratio according to the imposed value of the surface tension, $\gamma = 0$. After equilibration, data were collected over 50,000 DPD-MC cycles, at $\gamma = 0$. The statistical averages of the quantities of interest (see Method of Calculation of Statistical Quantities, below) were then made over configurations, which were separated from one another by 50 DPD steps. On average, 10,000 independent configurations were considered for the calculation of each of the statistical averages.

Method of calculation of statistical quantities

We have studied the physical properties of the model system both in the absence and in the presence of the proteins. The pure lipid bilayer hydrophobic thickness, $d_{\mathrm{L}}^{\mathrm{o}}$, was estimated by calculating the difference between the average position along the bilayer normal (i.e., the z direction, if one considers the bilayer parallel to the x,y plane) of the tail-beads attached to the headgroup (beads 4 and 9, as illustrated in Fig. 2) of the lipids in one (*top*) monolayer, and of the lipids in the opposite (*bottom*) monolayer,

$$d_{\mathrm{L}}^{\mathrm{o}} = \langle \overline{z_{\mathrm{t}}}^{(\mathrm{top})} - \overline{z_{\mathrm{t}}}^{(\mathrm{bottom})} \rangle, \tag{14}$$

where z_{t} is the z position of either bead 4 or 9 (Fig. 2) of the lipid. The *overline* indicates an average over the two chains for each lipid, and over the total number of lipids in each monolayer. The difference between the two terms in the above expression is further averaged over the number of the ensemble configurations.

To study the effect of a protein on the surrounding bilayer structure, we have calculated the lipid-bilayer hydrophobic thickness, $d_{\mathrm{L}}(r)$, as a function of the radial distance r from the protein hydrophobic surface, that is, at the interface with the lipid hydrocarbon chains, as schematically illustrated in Fig. 1 *d*. The method of calculation of $d_{\mathrm{L}}(r)$ resembles the one used to calculate $d_{\mathrm{L}}^{\mathrm{o}}$, as illustrated in Fig. 3. For each configuration, we have first calculated the circularly averaged value of the positions along the bilayer normal of the tail-beads attached to the headgroup of the lipids within each circular sector k ($k = 1,2,3,\ldots$) at distance $r = k\Delta r$ from the protein surface. The bin size Δr was chosen to be of the order of the diameter of the lipid projected area on the bilayer plane. This was done for both monolayers of the bilayer. The instantaneous value of the bilayer hydrophobic thickness at distance r from the protein surface is then given by the difference of these two values. To obtain $d_{\mathrm{L}}(r)$, this difference has been further averaged over all the sampled configurations, as

$$d_{\mathrm{L}}(r) = \langle \overline{z_{\mathrm{t}}}^{(\mathrm{top})}(r) - \overline{z_{\mathrm{t}}}^{(\mathrm{bottom})}(r) \rangle. \tag{15}$$

It is worth noticing that, if the protein is tilted (Fig. 3 *b*), the circular sectors (one at the top and the other at the bottom monolayer of the bilayer) at a distance r from the protein surface, are shifted in the bilayer plane with respect to each other. Therefore, the value of $d_{\mathrm{L}}(r)$ calculated by the method just described is an approximated value of the value of the actual bilayer thickness in the vicinity of the tilted protein. However, at sufficiently long distance from the protein, the calculated bilayer thickness converges to its actual bulk value. We also want to point out that because of the way in which $d_{\mathrm{L}}(r)$ is calculated, for the case of a tilted protein, possible effects from asymmetry of the protein orientation in the bilayer are averaged out.

The behavior of $d_{\mathrm{L}}(r)$ allowed us to access the extension of the protein-mediated perturbation on the bilayer. Based on a previous theoretical finding (Sperotto and Mouritsen, 1991), we first assumed that the perturbation induced by the protein on the surrounding lipids is of an exponential type. We have then verified this assumption later by analyzing the deviation of the functional form of the calculated $d_{\mathrm{L}}(r)$ from the one assumed. If the behavior of $d_{\mathrm{L}}(r)$ is exponential, the protein-induced perturbation can be expressed in terms of a typical coherence length, i.e., the decay length ξ_{P},

$$d_{\mathrm{L}}(r) = d_{\mathrm{L}}^{\mathrm{o}} + (d_{\mathrm{P}} - d_{\mathrm{L}}^{\mathrm{o}})e^{-\mathrm{r}/\xi_{\mathrm{P}}}, \tag{16}$$

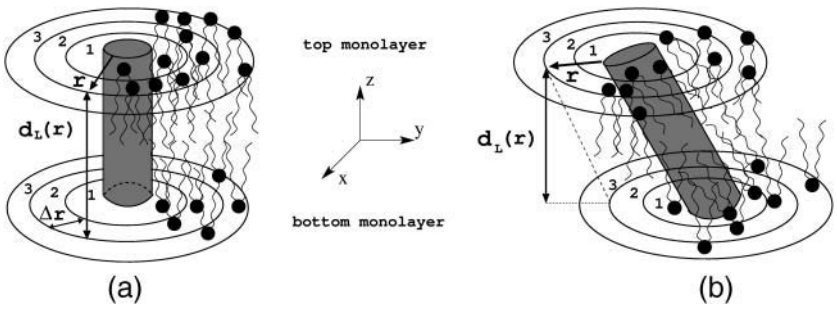

FIGURE 3 Schematic drawing to illustrate the method of calculation of $d_{\mathrm{L}}(r)$, which is described in detail in the text. The protein is represented by a shaded cylinder. The figure shows the case when the protein is parallel to the bilayer normal (*a*), and the case when the protein is tilted with respect to the bilayer normal (*b*).

where d_L^o is the mean hydrophobic thickness of the unperturbed pure lipid bilayer, and d_P is the protein hydrophobic length. The above equation expresses the fact that away from the protein surface, and at distances at least of the order of ξ_P, the perturbed $d_L(r)$ decays to the bulk value d_L^o, namely the value corresponding to that of the pure lipid system at the considered temperature, at least if no finite-size effects occur. In principle, by knowing $d_L(r)$, d_P, and d_L^o, and by using Eq. 16, one can estimate ξ_P. In our case we have determined the value of ξ_P by best-fitting with Eq. 16 the values $d_L(r)$ resulting from the simulations, where ξ_P and d_L^o are the fitting parameters. For the resulting value of the parameter d_L^o obtained by the best-fitting, we have verified that this is equal, within statistical accuracy, to the value of the lipid bilayer hydrophobic thickness in the bulk, which we directly calculated from the simulations. Since the proteins can be subjected to tilt, the input parameter for d_P we used is not the actual hydrophobic length of the model-protein, but instead an effective length, d_P^{eff}. The value d_P^{eff} is defined as the projection onto the normal of the bilayer plane of the protein hydrophobic length directly obtained from the simulations: $d_P^{eff} = d_P \cos(\phi^{tilt})$, where ϕ^{tilt} is the tilt-angle (see Fig. 1 *d*). The degree of tilting of a protein with respect to the bilayer normal was computed by considering, for each bead-chain forming the protein, the vector that connects the position of the two hydrophobic beads bound to the protein hydrophilic beads (i.e., close to the lipid-water interface), one located in one monolayer of the bilayer, and the other in the opposite monolayer. The tilt-angle, ϕ^{tilt}, is then defined as the average value, over all the chains forming the protein, of the angle between this vector and the bilayer normal.

In some cases, to facilitate the interpretation of the data obtained from the simulations, it was necessary to know the degree of order/disorder of the lipid chains in the vicinity of the protein, and eventually to compare it with that of the pure lipid bilayer, i.e., in the bulk, away from the protein-induced perturbation. Therefore, we have calculated the value of the lipid chain order parameter, $S(r)$, which is defined as

$$S = \frac{1}{2}\,(3\cos^2\phi_S - 1), \tag{17}$$

with

$$\cos\,\phi_S = \frac{\mathbf{r}_{ij}\cdot\hat{\mathbf{n}}}{r_{ij}} = \frac{z_{ij}}{r_{ij}}, \tag{18}$$

where ϕ_S is the angle between the orientation of the vector $\mathbf{r}_{ij} = \mathbf{r}_j - \mathbf{r}_i$ ($r_{ij} = |\mathbf{r}_{ij}|$) along two consecutive lipid chain beads, *i*,*j*, and the bilayer normal unit vector, $\hat{\mathbf{n}}$. S has the value of 1 if $\mathbf{r}_{ij}$ is on average parallel to the bilayer normal, 0 if the orientation is random, and -0.5 if the bond is on average parallel to the bilayer plane. The value $S(r)$ has been independently calculated for each of the two monolayers of the bilayer, as well as averaged over all the bonds of the lipid chains at distance r from the surface of the protein.

The details regarding the number of configurations used to estimate the statistical quantities were mentioned at the end of Statistical Ensemble and Surface Tension, above.

RESULTS AND DISCUSSION

In this section, we present the results from the simulations of the pure-DMPC lipid bilayer model system and the bilayer with embedded proteins. We have focused on the low protein-concentration regime, where the correlation between different proteins can be neglected. Therefore we considered bilayers with just a single embedded protein. To investigate the dependence on mismatch and protein size of the extension of the lipid bilayer perturbation around an embedded protein, we first studied the behavior of the system at a constant temperature, well above the pure lipid bilayer main-transition, or melting, temperature. Because one of the ways to change the hydrophobic mismatch is by changing temperature, we then studied the temperature-dependence of ξ_P and ϕ^{tilt} in the temperature range above the melting temperature of the pure system, i.e., in the fluid phase. We did this for a number of lipid-protein model-systems.

For convenience, in the following sections, together with the given values of the reduced temperatures, T^*, we have also added in brackets the corresponding approximated values in °C, estimated using Eq. 12. Because, as already stated, a direct mapping between the atomic level information and the model parameters is not possible, the values of the temperatures derived from the temperature-mapping previously described will also reflect this limitation. Therefore, in the following, the temperatures given in °C should be considered simply as general guidelines to which thermodynamic phase a system is in, at a given reduced temperature.

The results presented here refer to lipid bilayers composed of 900 lipids and 25 water beads per lipid, resulting in fully hydrated bilayers. The choice of 25 water beads per lipid was sufficient to ensure that the hydrophilic parts of the model protein would be fully hydrated even when the protein is not subjected to tilt. We have made calculations for smaller system sizes, and we have found that the chosen system size was sufficient to avoid finite-size effects, at least in the temperature range close or above the main-transition temperature of the pure bilayer system.

Pure lipid bilayer

Fig. 4 shows the phase behavior of the pure lipid bilayer hydrophobic thickness, d_L^o, as a function of reduced temperature T^*. The system undergoes a main transition at a reduced melting temperature $T_m^* = 0.425$, which is calculated from the inflection point of $d_L^o(T^*)$. This value of the melting temperature corresponds to the main-transition temperature of DMPC, which is ~24°C (Koynova and Caffrey, 1998). Above T_m^* the lipid chains are in the melted state, hence the low value of d_L^o, and the system is in the so-called L_α, or fluid phase. The snapshot in Fig. 4 (*bottom*, *right*) shows a typical configuration of the system in the fluid phase. For sake of clarity, in this, as well as in all snapshots shown in this article, the water molecules are not shown. At very low temperatures the system is in the so-called $L_{\beta'}$ or gel phase, which is characterized by having ordered chains, hence the high value of d_L^o. In this phase the lipid chains are tilted with respect to the bilayer normal. A typical configuration at this temperature can be seen in the snapshot in Fig. 4 (*bottom*, *left*).

When the temperature is increased above $T^* = 0.35$ (13.5°C), but is below T_m^*, a third phase occurs between the L_α and the $L_{\beta'}$ phases. This phase, which disappears again as the temperature reaches the main-transition temperature, is characterized by having striated regions, made of lipids in the gel-state, intercalated by regions made of lipids in the

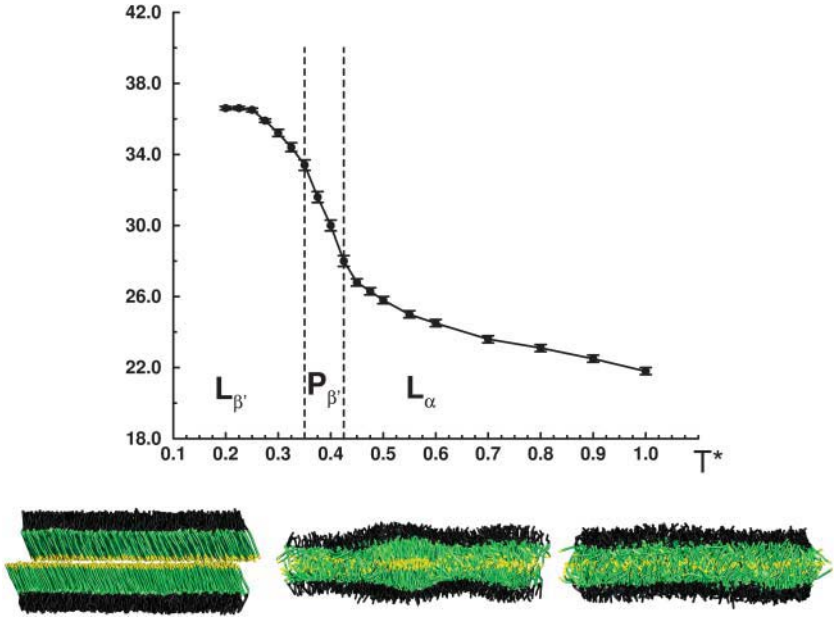

FIGURE 4 The pure lipid bilayer hydrophobic thickness, d_L^o, as a function of reduced temperature T^* (*top*). The main-transition temperature of the pure system is at the reduced temperature $T^* = 0.425$. Also shown are snapshots of typical configurations of the system simulated at reduced temperatures: $T^* < 0.35$, corresponding to gel-phase, or $L_{\beta'}$ (*bottom*, *left*); $0.425 > T^* \geq 0.35$, corresponding to the ripplelike striated phase, which here we denote as $P_{\beta'}$ phase (*bottom*, *center*); and $T^* > 0.425$, corresponding to the L_α or fluid phase (*bottom*, *right*). The lipid headgroups are represented by black lines, the lipid tails by green lines, and the end-segments of the lipid tails are shown in yellow.

fluid-state. This modulated structure can be seen in the snapshot in Fig. 4 (*bottom*, *center*). The striated phase, described in detail elsewhere (Kranenburg et al., 2004c), resembles the $P_{\beta'}$, or ripple-phase. The ripple-phase occurs in phospholipid bilayers above the pretransition temperature—which in the case of DMPC is ~14°C (Koynova and Caffrey, 1998)—and is characterized by a rippling of the bilayer, with a wavelength of the order of 150 Å (Canningham et al., 1998).

Using the scaling relation in Eq. 12, and the value of $R_c = 6.46$ Å for the conversion factor for the unit of length (see Length-, Time-, and Temperature-Scales, above), we can now compare the values of the bilayer hydrophobic thickness, and the area per lipid, obtained from our simulations with those referring to the fully hydrated DMPC bilayers, which are derived from experiments. Both sets of values are shown in Table 2. The values obtained from the simulations are in good quantitative agreement with the experimental data. Small deviations from the experimental values are only observed in the case of the area per lipid at high temperature (65°C), and in the case of the bilayer hydrophobic thickness in the gel phase (10°C).

Bilayers with embedded proteins

Fluid phase at a temperature well above melting temperature

The results discussed below refer to the reduced temperature $T^* = 0.7$ (60°C), well above the melting temperature of the system, i.e., in the fluid phase. The pure lipid bilayer hydrophobic thickness calculated at this reduced temperature is $d_L^o = 23.6 \pm 0.2$ Å. To study mismatch effects, we have considered proteins modeled by hydrophobic bead-chains made by a number of beads ranging from 4 to 12. To have an idea of what these numbers correspond to in terms of protein hydrophobic length, one can consider that the equilibrium distance between the beads is $r_{eq} = 0.7\ R_c$ (see Eq. 3); therefore the resulting values for the protein hydrophobic lengths will be $\tilde{d}_P = 14$ Å (4 beads), 18 Å (5 beads), 23 Å (6 beads), 32 Å (8 beads), 41 Å (10 beads), and 50 Å (12 beads). It is worth mentioning that these estimated protein hydrophobic lengths—which we denoted by $\tilde{d}_P$ to distinguish them from the protein hydrophobic lengths calculated from the simulations, and denoted by d_P—are only meant to be indicative. Because of the soft interactions involved in the DPD dynamics, the value of the protein hydrophobic length that results from the simulations, d_P, might be subjected to a small deviation of the order of 1 Å with respect to the values given above.

TABLE 2 Values obtained from the simulations and from experiments of the pure bilayer hydrophobic thickness, d_L^o, and area per lipid, A_L, of DMPC

		d_L^o [Å]		A_L [Å^2]	
T [°C]	Phase	Simulation	Experiment	Simulation	Experiment
10	$L_{\beta'}$	34.3	30.3*	48.6	47.2*
30	L_α	26.3	25.6†	60.4	60.0†
50	L_α	24.3	24.0†	64.4	65.4†
65	L_α	23.6	23.4†	65.7	68.5†

The data refer to temperatures both above and below the main-transition temperature, $T_m = 24$°C (Koynova and Caffrey, 1998).
*From Tristram-Nagle et al. (2002). The error for d_L^o is 0.2 Å, and for A_L 0.5 Å^2.
†From Petrache et al. (2000a). The error is not reported in the cited reference.

Fig. 5 shows the calculated bilayer hydrophobic thickness profile, $d_L(r)$, as a function of the distance r from the protein surface. The data refer to the different values of d_P, resulting in different values of hydrophobic mismatch Δd, ranging from $\Delta d = -8$ to 28 Å, and to the three protein sizes, which correspond to $N_P = 4$, 7, and 43. Because the probability of finding a lipid molecule in the lipid-shell closest to the protein (namely at the position $r = n\Delta r$ with $n = 1$) is much lower than in the other lipid-shells (with $n > 1$), the data collected at a distance $r = \Delta r$ from the protein surface have not been considered for the statistics. One can clearly see from the curves in Fig. 5 that the protein induces a perturbation of the lipid bilayer in its vicinity. The perturbation decays in a manner that depends on the hydrophobic mismatch, and on protein size. If the protein hydrophobic length is smaller than the unperturbed bilayer hydrophobic thickness ($d_P < d_L^o$), i.e., at negative mismatch $\Delta d < 0$ (*open symbols* in Fig. 5), to reduce exposure of the protein hydrophobic region to the water environment, the lipids around the protein shrink to match the protein hydrophobic surface. By choosing the peptide hydrophobic length to approximately match the value of the hydrophobic thickness of the unperturbed lipid bilayer, i.e., $\Delta d \approx 0$, one can clearly see from Fig. 5 (*crosses*) that the perturbation induced by the protein on the surrounding lipids becomes negligible. Instead, when the chosen protein is such that $d_P > d_L^o$, i.e., at positive mismatch $\Delta d > 0$ (Fig. 5, *solid symbols*), the lipids in the vicinity of the protein, to match the protein hydrophobic surface, stretch and become more gel-like than the bulk lipids far away from the protein.

Fig. 6 shows the thickness profiles for two values of mismatch, $\Delta d = -10$ Å, and $\Delta d = 17$ Å, and for the three considered protein sizes. The open circles indicate the data obtained directly from the simulations, whereas the continuum line is obtained by best-fitting with the function in Eq. 16, where d_L^o and ξ_P are the fitting parameters (and where d_P^{eff} is the input parameter). For convenience, we have drawn a horizontal dashed line to indicate the value of the pure lipid bilayer hydrophobic thickness, d_L^o, calculated at the same reduced temperature considered for the simulations of the mixed systems. To help the interpretation of the data, the value of the protein hydrophobic length, d_P, directly calculated from the simulations, and of the protein hydrophobic length projected onto the normal to the bilayer plane, d_P^{eff}, are also plotted (*shaded* and *open areas*). The best fit is obtained with the values of the fitting parameters given in Table 3, for the three chosen protein sizes, and for varying values of mismatch, i.e., protein hydrophobic thickness.

At negative mismatch, there is no observed difference between d_P and d_P^{eff}, as can be seen by looking at Fig. 6, *a*, *c*, and *e*. This means that the orientation of the protein is perpendicular to the bilayer plane, hence $d_P = d_P^{eff}$. For positive mismatch, when the mismatch is too high to be

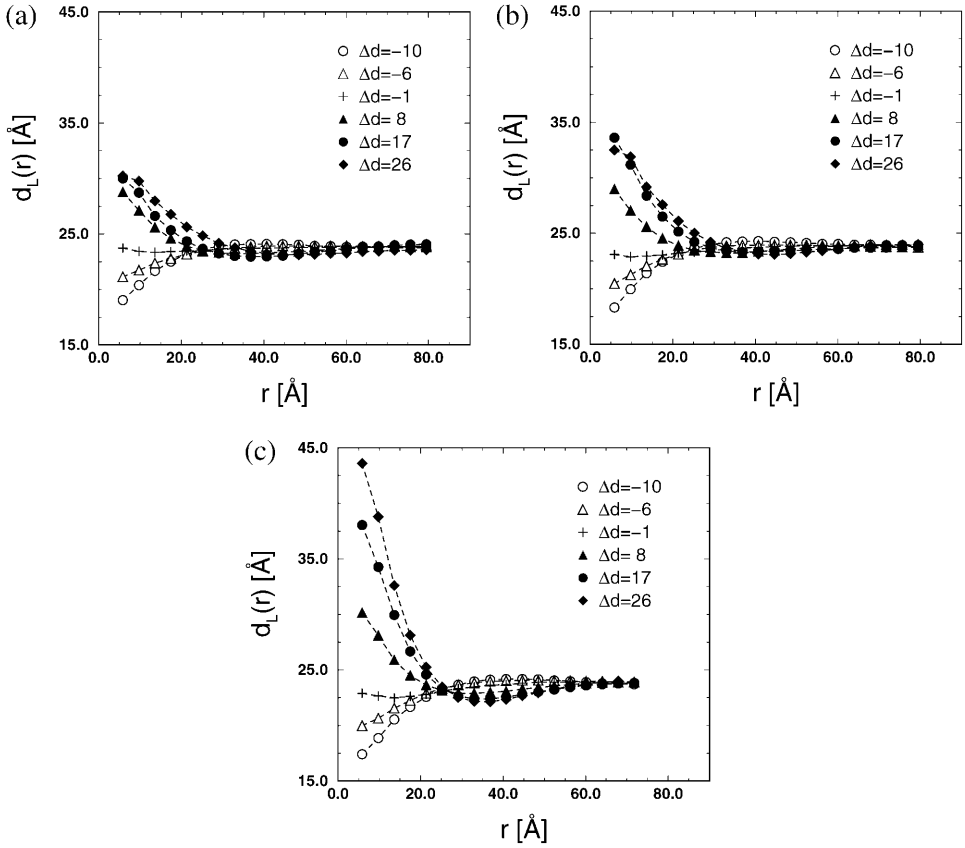

FIGURE 5 Lipid bilayer hydrophobic thickness profiles, $d_L(r)$, as a function of the distance r from the protein surface, for different hydrophobic mismatch, $\Delta d = \tilde{d}_p - d_L^o$, and for the three protein sizes corresponding to (*a*) $N_P = 4$, (*b*) $N_P = 7$, and (*c*) $N_P = 43$. The data refer to results from simulations made at the reduced temperature $T^* = 0.7$, which is well above the main-transition temperature of the pure system, $T_m^* = 0.425$. The calculated value of the pure lipid bilayer hydrophobic thickness at $T^* = 0.7$ is $d_L^o = 23.6 \pm 0.2$Å. The symbols for Δd refer to the following estimated values of the protein hydrophobic length: the open circle to $\tilde{d}_p = 14$ Å (negative Δd); the open triangle to $\tilde{d}_p = 18$ Å (negative Δd); the plus symbol to $\tilde{d}_p = 23$ Å ($\Delta d \approx 0$); the solid triangle to $\tilde{d}_p = 32$ Å (positive Δd); the solid circle to $\tilde{d}_p = 41$ Å (positive Δd); and the solid diamonds to $\tilde{d}_p = 50$ Å (positive Δd).

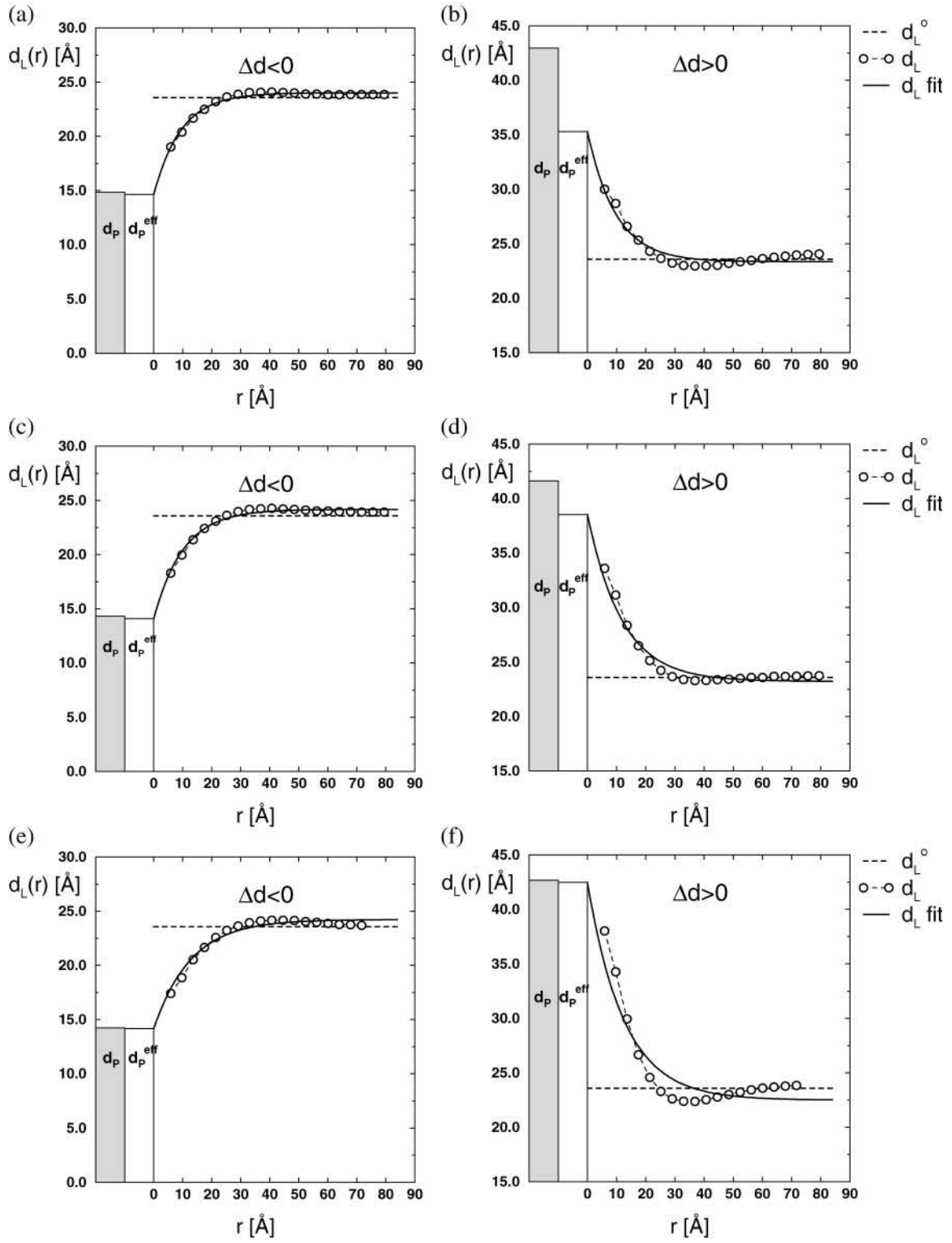

FIGURE 6 Calculated values of $d_L(r)$ (*open circles*) and fitted values using Eq. 16 (*solid line*) as a function of the distance r from the protein surface. The data refer to the three protein sizes $N_P = 4$ (*a*,*b*), $N_P = 7$ (*c*,*d*), and $N_P = 43$ (*e*,*f*), and to two values of the protein hydrophobic length $d_P = 14$ Å ($\Delta d = -10$ Å) and 41 Å ($\Delta d = 17$ Å). Also shown is the level value of the pure lipid bilayer thickness, $d_L^o = 23.6 \pm 0.2$ Å (*dashed line*), the measured protein hydrophobic length d_P (*shaded area*), and the effective protein hydrophobic length d_P^{eff} (*open area*), which is defined as the projection of d_P onto the normal to the bilayer plane. The data refer to simulations at the reduced temperature $T^* = 0.7$.

TABLE 3 Values of the decay length, ξ_P; the pure lipid bilayer hydrophobic thickness d_L^o (both derived from fitting the thickness profiles $d_L(r)$ by using Eq. 16); the protein hydrophobic length, d_P; and the effective protein hydrophobic length, d_P^{eff} (both calculated from the simulations) given for different values of hydrophobic mismatch, Δd, and for the three protein sizes corresponding to $N_P = 4$, 7, and 43

Protein	Δd [Å]	ξ_P [Å] Fitted	d_L^o [Å] Fitted	d_P [Å] Computed	d_P^{eff} [Å] Computed
$N_P = 4$	−10	9.3 ± 0.3	24.0 ± 0.1	15 ± 1	15 ± 1
	−6	11.9 ± 0.3	23.9 ± 0.1	19 ± 1	19 ± 1
	−1	—	—	24 ± 1	24 ± 1
	8	9.6 ± 0.7	23.4 ± 0.1	33 ± 1	32 ± 1
	17	9.7 ± 0.7	23.4 ± 0.2	42 ± 1	35 ± 3
	26	12.3 ± 0.6	23.2 ± 0.1	51 ± 1	36 ± 3
$N_P = 7$	−10	10.1 ± 0.4	24.2 ± 0.1	15 ± 1	14 ± 1
	−6	12.4 ± 0.7	24.0 ± 0.1	19 ± 1	19 ± 1
	−1	—	—	24 ± 1	23 ± 1
	8	9.4 ± 0.8	23.5 ± 0.1	33 ± 1	32 ± 1
	17	11.8 ± 0.7	23.2 ± 0.2	42 ± 1	39 ± 2
	26	12.4 ± 0.8	23.3 ± 0.2	51 ± 1	39 ± 3
$N_P = 43$	−10	12.8 ± 0.8	24.2 ± 0.1	14 ± 1	14 ± 1
	−6	17 ± 2	24.3 ± 0.2	19 ± 1	19 ± 1
	−1	—	—	24 ± 1	24 ± 1
	8	10 ± 1	23.2 ± 0.3	33 ± 1	33 ± 1
	17	12 ± 1	22.5 ± 0.6	42 ± 1	43 ± 1
	26	12 ± 1	22.1 ± 0.8	51 ± 1	51 ± 2

The data refer to simulations made at the reduced temperature $T^* = 0.7$, well above the main-transition temperature of the pure lipid bilayer system. The pure lipid bilayer hydrophobic thickness calculated at this temperature is $d_L^o = 23.6 \pm 0.2$ Å. In the case of ~0 mismatch ($\Delta d = -1$ Å), the values of ξ_P and d_L^o are not calculated.

compensated for by fully stretching the lipids in the vicinity of the protein, another effect can be observed: the peptide tilts to decrease its effective hydrophobic length. The effect is much more pronounced in the case of the skinny protein ($N_P = 4$) than for the larger protein, as can be seen by comparing Fig. 6 *b* with Fig. 6 *d* and Fig. 6 *f*, where, in the former cases, d_P^{eff} is much shorter than the actual protein hydrophobic length. The values of d_P^{eff} and d_P, reported in Table 3, show that this tilt-dependence on protein size is also valid for the other values of positive mismatch.

The derived values of ξ_P (using Eq. 16) as a function of protein size and hydrophobic mismatch, which are shown in Table 3, indicate that there is a mismatch-dependence of the perturbation caused by the protein on the surrounding lipids. For a given protein size, N_P, if the mismatch is negative, the correlation length increases with decreasing mismatch (absolute value), whereas for positive mismatch the opposite happens, and the correlation length increases with increasing mismatch. Also, in the case of $\Delta d < 0$ the decay length increases by increasing the protein size. Instead there is no detectable ξ_P dependence on Δd in the case of $\Delta d > 0$, at least at the considered temperature, i.e., well above the melting temperature of the pure system. The scenario is somehow different when the temperature decreases and approaches the transition temperature, as will be discussed in detail in the next section.

In one specific case, our simulation data may be quantitatively compared with the data obtained from MD simulations on an all-atom model. Jensen and Mouritsen (2004) calculated the decay length from MD simulations in bilayers of fluid palmitoyloleoylphosphatidylethanolamine and palmitoyloleoylphosphatidylcholine with the membrane channel aquaglyceroporin embedded. Their system would correspond to a protein size $N_P = 43$, and to a negative mismatch of ~−4 Å. The MD simulations predicted that when the hydrophobic length of the protein is shorter than the pure lipid bilayer hydrophobic thickness, the lipids close to the lipid-protein interface compress to favor hydrophobic matching—thus inducing a curvature in the bilayer. The mismatch-induced perturbation is of an exponential type and can be characterized by a decay length of ~10 Å. This value is in good agreement with the value predicted by our simulations (see Table 3). Also, simulations on palmitoyloleoylphosphatidylcholine bilayers that had a much smaller protein embedded than aquaglyceroporin, i.e., the membrane channel gramicidin A, predicted that this channel induces perturbation with a coherence length smaller than that obtained for aquaglyceroporin (M. Ø. Jensen, private communication).

At the present stage of experimental development, it is difficult to correlate in a systematic way the extent of the perturbation induced by proteins with the hydrophobic mismatch, or the protein size. There are few experimental quantitative estimates of the range of the perturbation that some specific proteins, such as bacteriorhodopsin (Rehorek et al., 1985; Bryl and Yoshihara, 2001), lactose permease (Lehtonen and Kinnunen, 1997), and the synthetic α-helical peptides (Ridder et al., 2004; Weiss et al., 2003), may induce

on reconstituted pure lipid bilayers. The results from these experiments suggest that the perturbation might be mismatch- and protein-size-dependent; i.e., the larger the protein, the more long-range the perturbation. There are also indirect evidences that point out that the coherence length associated to the protein-induced perturbation is dependent on protein size. It was suggested (Ridder et al., 2004) that, if this dependence occurs, bilayer activities affected by changes of the coherence length might also be affected by changing the protein size. This is certainly the case for the phenomenon of *flip-flop* of phospholipids in bilayers. In fact, the experimental data on flip-flop suggest that the larger the protein size (and therefore the smaller its curvature at the interface with the lipid chains), the more reduced the ability of the protein to cause flip-flop (Kol et al., 2003). Our theoretical predictions for the decay-length dependence on protein-size and mismatch are consistent with these few experimental data available.

Also, for the large protein with $N_P = 43$, the lipid thickness profile around the protein differs from an exponential one, as shown in Fig. 6, *e* and *f*. The effect is even more pronounced at lower temperatures (data not shown), at least in the case of negative mismatch (since lower temperature means larger negative mismatch). The non-exponential behavior, and the possible reason for it, will be discussed later. In Table 3 are also given the values of the pure lipid bilayer hydrophobic thickness, d_L^o (*fitted*), obtained from the best fit (using Eq. 16) of the values of the thickness profiles, $d_L(r)$, obtained from the simulations. For all the considered cases, the values of d_L^o (*fitted*) compares well with the value of the pure lipid bilayer hydrophobic thickness, $d_L^o = 23.6$ Å, obtained directly from the simulations at the considered temperatures.

We now discuss the protein-tilt issue. The calculated protein tilt-angle with respect to the bilayer normal as a function of Δd and protein size, N_P, is shown in Fig. 7. For $\Delta d < 0$ the tilt-angle is $\sim 10°$. One should consider that this value corresponds to an extremely small tilt; in fact, 10° is within the statistical tilt-fluctuations to which the model protein is subject during the simulation. As the protein hydrophobic length increases (and the mismatch becomes positive), the protein undergoes a significant tilting. Also, for equal values of hydrophobic mismatch, the thinner protein ($N_P = 4$) is much more tilted than the fatter one ($N_P = 43$). These results suggest that, when the protein is small, the main mechanism to compensate for a large hydrophobic mismatch is the tilt, whereas large proteins react to negative mismatch by causing an increase of the hydrophobic thickness of the nearby bilayer. This is clearly illustrated by the snapshots in Fig. 7 (*right*). These snapshots show typical configurations of the system, at the considered reduced temperature, $T^* = 0.7$ (60°C), for the three protein sizes, $N_P = 4$, 7, and 43, and for the highest (positive) value of mismatch, $\Delta d = 26$ Å.

Theoretical studies based on MD simulations on all-atom models have pointed out the possibility that α-helical hydrophobic peptides may tilt when subjected to positive mismatch conditions (Shen et al., 1997; Belohorcová et al., 1997; Petrache et al., 2002), and that the degree of tilting may depend on the specific system, i.e., on the chosen peptides. Despite the limited timescale sampled by MD simulations, the predictions made by these all-atom model studies have been confirmed by experimental studies. In fact, the results from very recent experimental investigations by solid-state nuclear magnetic resonance (NMR) spectroscopy (Strandberg et al., 2004) show that α-helical synthetic peptides—of fixed hydrophobic length, and with a hydrophobic leucine-alanine core and tryptophan flanked ends—experience a small tilting when embedded in phospholipid bilayers of varying hydrophobic thickness

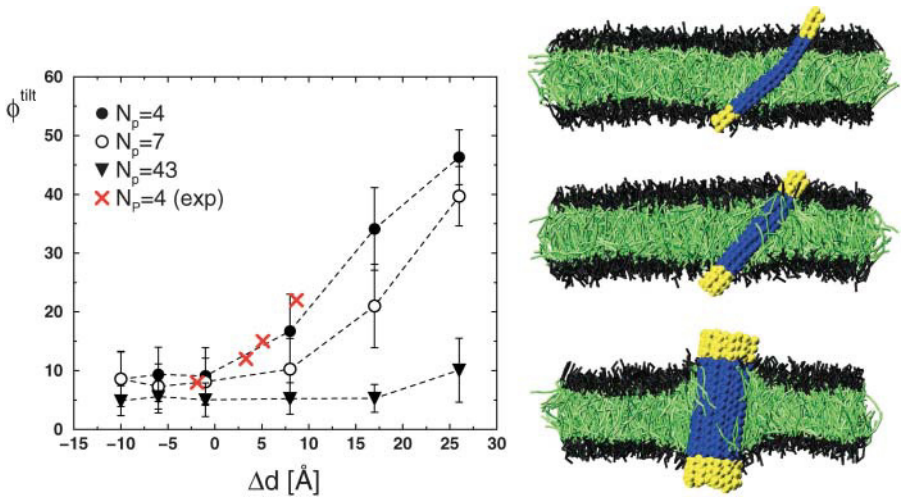

FIGURE 7 The protein tilt-angle, ϕ^{tilt}, dependence on mismatch, $\Delta d = \bar{d}_p - d_L^o$ (i.e., different protein hydrophobic lengths). The data refer to simulations made at the reduced temperature $T^* = 0.7$. The calculated pure lipid bilayer hydrophobic thickness at this temperature is $d_L^o = 23.6 \pm 0.2$ Å. The data are given for the three considered protein sizes $N_P = 4$, 7, and 43. The dashed lines are only a guide for the eye. The crosses in red are the rescaled experimental values (Koehorst et al., 2004) of the tilt-angle experienced by the M13 coat protein peptide embedded in phospholipid bilayers of varying hydrophobic thickness. Typical configurations of the systems resulting from the simulations are shown on the right. Starting from the top, the snapshots refer to proteins sizes $N_P = 4$, 7, and 43, respectively. In the three cases the protein hydrophobic length is $\bar{d}_p = 50$ Å, hence the hydrophobic mismatch is $\Delta d = 26$ Å.

(such that $d_P \geq d_L^o$, i.e., $\Delta d > 0$). It was found that the tilt-angle systematically increases by increasing hydrophobic mismatch; however, the tilt-dependence on hydrophobic mismatch was not as pronounced as one would have expected for a given mismatch. This result brought the authors to conclude that the tilt of these peptides is energetically unfavorable, and to suggest that the anchoring effects by specific residues such as tryptophans are more dominant than mismatch effects. That the actual value of the tilt-angle might be dependent on local features, such as the specific helix sequence of the peptides, is indeed confirmed by the results obtained from a site-directed fluorescence spectroscopy experiment by Koehorst et al. (2004). These authors correlated systematically data on the tilt experienced by the M13 major coat protein (α-helical) peptide when embedded in fluid, unsaturated phospholipid bilayers of varying hydrophobic thickness, with the hydrophobic mismatch (positive and negative). It was found that for values of mismatch of the same order as that experienced by the synthetic peptides mentioned above (Strandberg et al., 2004), the degree of tilting experienced by the M13 peptide is much higher. However, as for the case of the synthetic peptides, the tilt-angle increases by increasing the mismatch (Koehorst et al., 2004). Our simulation data show a well-defined dependence of the protein tilt-angle on hydrophobic mismatch. In an attempt to see if the tilt-dependence on mismatch derived from the simulation data bears some resemblance to the experimental one, in Fig. 7 we have also shown (*red crosses*) the experimental data of Koehorst et al. (2004). To compare the experimental dependence with the one obtained from the simulations, we have shifted all the experimental tilt-values by a fixed amount (11°). The red crosses in Fig. 7 show that, within the statistical errors, the dependence predicted from the simulations is in good agreement with that experimentally predicted, at least in the mismatch range considered by the experiments.

Incidentally, the results from our simulations suggest that, when a skinny peptide ($N_p = 4$) is subjected to a high positive mismatch ($d_P > d_L^o$), it might bend, in addition to experiencing a tilt, as can be seen by looking at the snapshot shown in Fig. 7 (*top*, *right*). Also, as soon as the positive mismatch decreases, the bending disappears, although the peptide tends to remain tilted. Results from MD simulations on an all-atom model of a poly(32)alanine helical peptide embedded in a DMPC bilayer show that this type of helix not only tilts by 30° as a whole with respect to the bilayer normal, but also experiences a bend in the middle (Shen et al., 1997); MD simulations have also shown a similar tendency for a poly(16)leucine helical peptide embedded in a DMPC bilayer (Belohorcová et al., 1997). From the experimental point of view it is now possible to detect peptide-protein bending by NMR spectroscopy (Nevzorov et al., 2004; Strandberg et al., 2004). Indeed, the data from Strandberg et al. (2004), for the behavior of a synthetic leucine-alanine α-helical peptide in lipid bilayers of varying thickness, do indicate that at high positive mismatch the peptides might experience bending in addition to tilting, in agreement with our predictions. However, we must add that the occurrence, or extent, of bending in the small peptide ($N_p = 4$) might very well be dependent on the value of the bending constant, K_θ (see Eq. 5), chosen for the simulations.

Fluid phase at temperatures approaching the melting temperature from above

We now discuss the response of the lipid-protein system when the temperature decreases and approaches the main-transition temperature. The dependence of ξ_P on the reduced temperature, T^*, with $T^* > T^*_m$, is shown in Fig. 8, for two values of protein hydrophobic length $\tilde{d}_P = 14$ Å, and $\tilde{d}_P = 41$ Å. These values were chosen to fulfill the condition that either $\Delta d < 0$ ($\tilde{d}_P = 14$ Å) or $\Delta d > 0$ ($\tilde{d}_P = 41$ Å), even if by changing the temperature, lipid bilayer hydrophobic thickness, and consequently Δd, may change. The data refer to two protein sizes, $N_P = 7$ and $N_P = 43$. The behavior of ξ_P shown in Fig. 8 indicates that, the closer the temperature to the main-transition temperature, the longer the perturbation caused by the protein on the surrounding lipids. This is probably due to the enhanced density fluctuations that occur

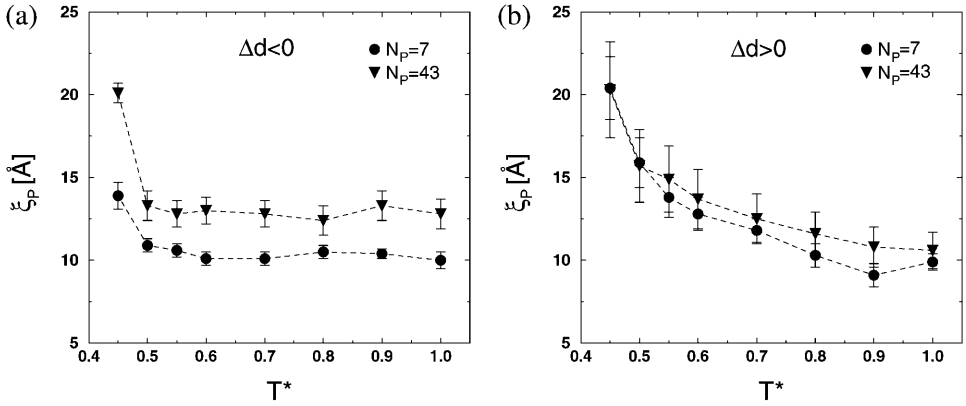

FIGURE 8 Decay length, ξ_P, dependence on reduced temperature T^*, ($T^* > T^*_m$), for two values of the protein hydrophobic length (*a*) $\tilde{d}_p = 14$ Å and (*b*) $\tilde{d}_p = 41$ Å. These values were chosen to guarantee that, in the considered range of temperatures, the mismatch is always either negative ($\tilde{d}_p = 14$ Å) or positive ($\tilde{d}_p = 41$ Å), even if by changing temperature the lipid bilayer hydrophobic thickness, and consequently Δd, may change. The data refer to two protein sizes corresponding to $N_P = 7$ and 43. The dashed lines are only a guide for the eye.

in the pure system close to the transition temperature. Also, for negative mismatch, there is a more pronounced dependence of ξ_P on the protein size than for positive mismatch, i.e., the larger the protein is, the longer the correlation length becomes. The dependence on protein size can be qualitatively explained by the fact that, the larger the protein, the smaller its curvature, and therefore the influence of a given portion of the protein hydrophobic surface extends to more lipids for larger proteins. Although for positive mismatch the dependence on protein size is not very pronounced, the values of ξ_P, in the case of the large protein, are systematically higher than those related to the small protein. These findings are in qualitative agreement with the results obtained from Monte Carlo simulations on lattice models (Sperotto and Mouritsen, 1991), which predicted that the temperature-dependence of the decay length has a dramatic peak at the transition temperature. Also, close to this temperature, it was found that the dependence of the decay length on the protein size was much enhanced. A quantitative comparison between our data and the data from the model study of Sperotto and Mouritsen (1991) would not be worthwhile, because the lattice model cannot account for tilting of the protein in response to mismatch. To our knowledge there are no experimental data available concerning the dependence of decay length on temperature.

It is worth mentioning that our model studies also predict that the larger the protein size, the more the behavior of $d_L(r)$ obtained from our DPD simulations differs from that of the exponential function used for the best fitting. This could already be seen by looking at Fig. 6 *f* in the case of $d_P > d_L^o$. Fig. 9 illustrates, in more detail, the non-exponential dependence on r of the lipid bilayer thickness profile. The figure shows the calculated values of $d_L(r)$ (*open circles*) and the fitted values (*solid line*) using Eq. 16. The data refer to a protein size $N_P = 43$, and to these two cases:

1. $\Delta d = -12$ Å ($\tilde{d}_P$=14 Å) and $T^* = 0.5$ (33.5°C),
2. $\Delta d = 19$ Å ($\tilde{d}_P$= 41 Å) and $T^* = 1.0$ (100°C).

In the case of positive and high mismatch ($d_P > d_L^o$), but at a rate low enough to avoid protein tilting, Fig. 9 *b* indicates that the lipids in the nearest shells to the protein surface are characterized by a gel-like chain to minimize the hydrophobic mismatch. Surprisingly, next to this lipid-ordered region, there appears a region (which, for convenience, we denote the *undershooting* region) consisting of a few lipid-shells, where the bilayer has a hydrophobic thickness less than that in the bulk. The undershooting phenomenon is probably due to the fact that, on the one hand, the system has to satisfy the constraint imposed by the value of the hydrophobic bilayer thickness of the bulk; and, on the other hand, the system has to adjust to the perturbation caused by the protein so as to hold the bilayer density constant, as well as close to the protein. We suggest that, if the protein is large enough that tilting is unfavorable, and if the mismatch is high enough that even the ordered (gel-like) lipids closest to the protein are not able to match the protein hydrophobic surface, a void is formed in the center of the bilayer. To fill the void and maintain the constraint of uniform density in the bilayer core, the lipid chains in the undershooting region might tend to tilt toward the protein. This hypothesis is indeed consistent with the fact that, although the end-to-end distance of the lipids in the undershooting region is approximately equal to the distance of the lipids in the bulk, the projected length on the bilayer normal is shorter than that of the lipids in the bulk. Therefore, in the undershooting region, the bilayer hydrophobic thickness is smaller than in the bulk. In the case of

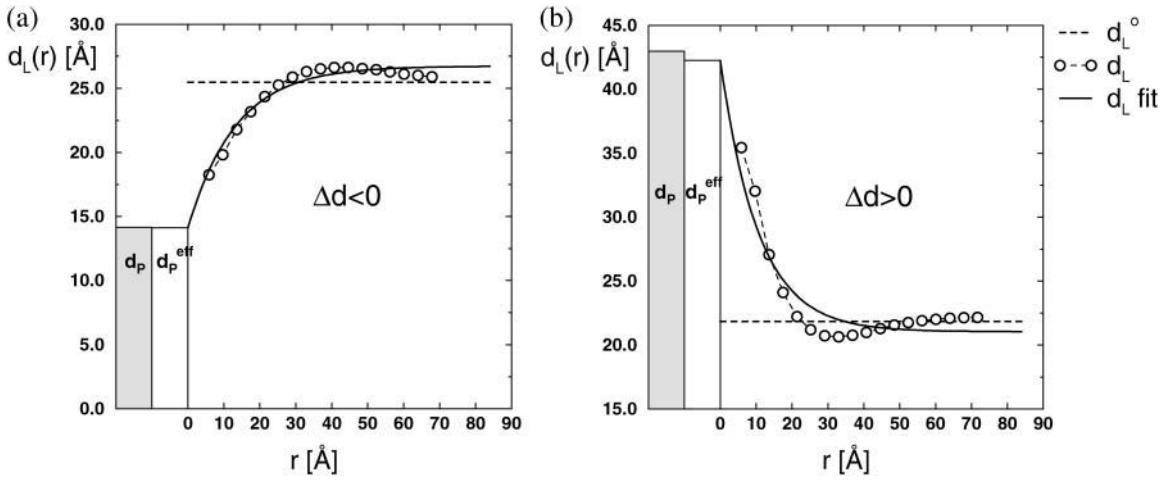

FIGURE 9 The calculated values of $d_L(r)$ (*open circles*) and the fitted values using Eq. 16 (*solid line*) as a function of the distance r from the protein surface. The data refer to a protein size of $N_P = 43$, and to the following cases: (*a*) $\tilde{d}_p = 14$ Å ($\Delta d = -12$ Å) and $T^* = 0.5$, and (*b*) $\tilde{d}_p = 41$ Å ($\Delta d = 19$ Å) and $T^* = 1.0$. Both values of temperature are above the melting temperature of the pure system. The dashed line indicates the value of the pure lipid bilayer hydrophobic thickness, d_L^o, at the considered temperature. Also shown are the measured protein hydrophobic length d_P (*shaded area*), and the effective protein hydrophobic length d_P^{eff} (*open area*), which is defined as the projection of d_P onto the normal to the bilayer plane.

$d_P < d_L^o$ (see Fig. 9 *a*), the bilayer in a neighboring region (which, in this case, we call the *overshooting* region) to that closest to the protein interface has a hydrophobic thickness higher than that of the lipid bilayer in the bulk. This might be explained by the fact that the lipid chains, nearest to the protein, tilt (and possibly bend) to satisfy the matching constraint, and, at the same time, the lipids in the overshooting region stretch their chains (i.e., become more gel-like) to satisfy the constant density constraint. This is consistent with the fact that, in the region closest to the protein (the so-called *annulus*), the values of the order parameter of the lipid chains, and of both the lipid end-to-end distance and projected length, are smaller than the values in the bulk. This shows that the lipids closest to the protein are more disordered and might bend to match the protein hydrophobic length (which is shorter than the bilayer thickness at the considered temperature). On the other hand, the projected length on the bilayer normal of the lipids in the overshooting region is slightly longer than that of the lipids in the bulk; and the order parameter, S, in the overshooting region is higher than in the bulk. This indicates that the lipids in this region are more stretched and ordered (i.e., gel-like) than the lipids in the bulk. To visualize the conformation of the lipids in the undershooting and overshooting regions, one could imagine that the lipids in the undershooting region are arranged as if forming a sector of an inverted micelle, whereas the lipids forming the *annulus* and the overshooting region are arranged as if forming a sector of a micelle. Furthermore, both for positive and negative mismatch, the behavior of $d_L(r)$ in Fig. 9 (*open circles*) at very low values of r might suggest that the protein-induced perturbation decays in a hyperbolic manner and with a flex point reasonably close to the protein surface. One could then speculate that this might reflect the onset of a wetting layer, which may expand to several lipid layers when appropriate physical conditions are present (Gil and Ipsen, 1997; Gil et al., 1998). A non-monotonic behavior of $d_L(r)$, similar to that seen in Fig. 9 *a*, was indeed predicted by studies on a phenomenological model (Nielsen et al., 1998), which described the lipid bilayer as a continuum elastic medium subjected to boundary conditions at the lipid-protein interface. The non-monotonic behavior of $d_L(r)$, observed by Nielsen et al. (1998), might occur for a different reason than the behavior causing the overshooting phenomenon shown in Fig. 9 *a*. A comparison between the results of these two models is difficult to make because, in the phenomenological model of Nielsen et al. (1998), the contact slope of the lipids nearest to the protein is a quantity that has to be assigned a priori; also, the phenomenological model does not allow for tilting of the protein as a whole, which is a result of the cooperativity of the system. Finally, we want to point out that the overshooting/undershooting effect shown in Fig. 9 seems not to be due to finite-size effects.

Concerning the dependence of the protein tilting on mismatch, one should recall that the hydrophobic mismatch condition can be varied either by changing the protein hydrophobic length or by changing temperature. As can be seen from Fig. 4, a change in temperature causes a change of the lipid bilayer hydrophobic thickness, hence of hydrophobic mismatch. In an attempt to understand whether temperature changes induce effects other than changes of mismatch, in Fig. 10 we have plotted the tilt-angles as a function of mismatch. The data refer to a number of lipid-protein systems; in fact we have plotted all possible hydrophobic mismatch values that resulted by considering either 1), the same lipid-protein system, but simulating it at different temperatures; or 2), by changing the protein hydrophobic length at fixed temperature (always above the main-transition temperature, i.e., in the fluid phase). A comparison between the curves shown in Fig. 7 and those shown in Fig. 10 shows that the functional dependence of the tilt-angle on mismatch is, within statistical accuracy, approximately the same in the two figures. This suggests that one can cause the same protein tilting either by changing the protein hydrophobic thickness or by changing the temperature. This means that, with respect to protein tilting, a change in temperature does not cause significant effects other than mismatch changes. In the case of the medium-size protein ($N_P = 7$), the data in Fig. 10 could suggest an oscillatory behavior of the tilt-angle as a function of mismatch. This would indicate that a change in temperature might cause other effects besides mismatch changes. However, because of the statistical accuracy of our data

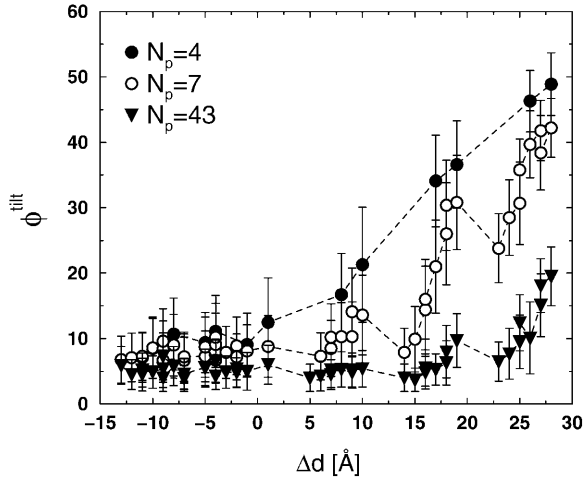

FIGURE 10 Protein tilt-angle, ϕ^{tilt}, as a function of the hydrophobic mismatch, $\Delta d = \tilde{d}_p - d_L^o$, and for the three protein sizes corresponding to $N_P = 4$, 7, and 43. Different hydrophobic mismatch conditions may be obtained either by varying protein hydrophobic length or temperature. The points in the curves refer either to the same lipid-protein system studied at different reduced temperatures or to different systems (i.e., lipid bilayers with a protein embedded whose hydrophobic length can be varied). The data shown in the figure are calculated at values of reduced temperatures above the main temperature of the pure system, $T_m^* = 0.425$ (i.e., in the fluid phase). The dashed lines are only a guide for the eye.

(see error bars), we cannot attribute the oscillatory behavior to effects others than mismatch.

CONCLUSION AND FUTURE PERSPECTIVES

In this article we have presented a mesoscopic model for lipid bilayers with embedded proteins. The model is based on the pure lipid bilayer mesoscopic model for DMPC, and was implemented to account for the presence of proteins embedded in the lipid bilayer. We have considered proteins of different hydrophobic length and different sizes. The lipid-protein bilayer model was studied at low protein/lipid ratios by mean of the DPD simulation method. The aim of our work was to understand whether, and to what extent—due to hydrophobic mismatch, and via the cooperative nature of the system—a protein may prefer to tilt (with respect to the normal to the bilayer plane), rather than to induce a bilayer deformation without (or even with) tilting. Therefore, we have systematically correlated the protein-induced perturbation and the lipid-induced protein tilting with different hydrophobic mismatch conditions. To our knowledge, this is the first attempt to draw such a correlation with the help of a mesoscopic model and the DPD simulation technique.

The results from our simulation studies are in qualitative good agreement with previous theoretical predictions concerning the dependence on mismatch and protein size, of the extent of the perturbation caused by the protein on the nearby lipids (Sperotto and Mouritsen, 1991; Jensen and Mouritsen, 2004). Also, they are in agreement with the few experimental quantitative estimates of the range of the perturbation that some specific proteins such as bacteriorhodopsin (Rehorek et al., 1985; Bryl and Yoshihara, 2001), lactose permease (Lehtonen and Kinnunen, 1997), and the synthetic α-helical peptides (Ridder et al., 2004; Weiss et al., 2003) induce on reconstituted pure lipid bilayers. In addition to perturbing the surrounding lipid matrix, proteins can also undergo a tilting to minimize the exposure of their hydrophobic moieties to the water environment. Therefore, we have also determined the dependence of the tilt-angle on mismatch. We found that, to adapt to a too-thin bilayer, the protein may tilt and even bend—in a manner that is mismatch- and protein-size-dependent (i.e., the larger the protein, the less pronounced the tilting). For the case of the skinny, peptidelike proteins, our results predict a functional dependence of the tilt on mismatch that is in good agreement with the one (see Fig. 7) recently found by spectroscopic measurements on unsaturated phospholipid bilayers that had the M13 major coat protein peptides embedded (Koehorst et al., 2004). Based on these results, one would be tempted to speculate that, whereas the actual values of the protein tilt-angle might depend on the specific peptide sequence, the functional dependence on mismatch might instead have a more general character. However, more experimental data are needed to validate this hypothesis. The importance of these studies on the inclination of proteins, or peptides, in lipid bilayers resides in the fact that knowing the physical causes of tilting can be useful in making predictions about protein transmembrane domains from protein sequences. Also, to study experimentally and/or theoretically the tilt-dependence on mismatch of isolated hydrophobic peptides may help us to understand whether the tilting of helices belonging to bundle proteins is due to an intrinsic property of the helices or is due, instead, to hydrophobic matching. This knowledge is biologically relevant, since there are experimental evidences suggesting that a mismatch-induced change of the tilt-angle of individual helices in channel bundle-proteins is the cause of changed protein activity (Lee, 2003).

The qualitative and quantitative agreement between our data and the data from previous theoretical or experimental studies have confirmed the reliability of the approach based on the application of the DPD simulation method on a mesoscopic model. Nevertheless, the aim of theoretical studies, such as the study presented here, is also to make predictions. Not only could these studies provide a possible framework for the interpretation of experimental data, but they could also be used as a complementary tool to experimental studies to reveal information not otherwise accessible, as well as serve as a source of inspiration for future experiments. Our simulation data suggest that, when the protein is small, the main mechanism to compensate for a large hydrophobic mismatch is the tilt, whereas large proteins react to negative mismatch by causing an increase of the hydrophobic thickness of the nearby bilayer. An interesting prediction is that, when the temperature of the system changes, the effect on the tilt is not from causes other than temperature-induced changes of the mismatch condition (see Fig. 10). This means that to cause the same degree of protein tilting, one can either change the protein, i.e., the protein hydrophobic length (hence the mismatch) or, more simply, change the temperature of the system in such a way as to tune the hydrophobic bilayer thickness to the value that one needs to have a well-defined mismatch. The same does not apply in the case of the mismatch effect on the decay length (data not shown). This is not that surprising, as the extent of the protein perturbation on the lipid bilayer is dependent on the lateral density fluctuations of the system, and these are known to be strongly enhanced in a range of temperature close to the main-transition temperature.

Another interesting theoretical prediction can be made in the case of large proteins, not subjected to tilt, and experiencing a high mismatch. In the vicinity of the protein, but further away from the so-called *annulus*, there might appear a few lipid-shells' worth of curved region—which we called the *undershooting* or *overshooting* region, depending on whether $d_P > d_L^o$ (positive mismatch) or $d_P < d_L^o$ (negative mismatch), respectively (see Fig. 9)—where the bilayer has a hydrophobic thickness that is lower (or higher) than the thickness found in the bulk, i.e., far away from the protein surface.

There could be a number of biological consequences if a curved structure, resulting from the overshooting/undershooting effect, forms around proteins embedded in biological membranes. On the one hand, its presence could affect the permeability of the membrane. When more than one lipid species is present in the system, it could induce a lipid-sorting in the vicinity of proteins and could also affect lipid-mediated protein-protein contacts, hence the protein lateral distribution, and it could create a fertile ground for the attachment of fusion peptides, which are known to enter the bilayer in a oblique manner (Brasseur, 2000; Lins et al., 2001), and thus could be favored by the presence of tilted lipids. But on the other hand, the formation of an overshooting/undershooting region could cause a change in the lateral pressure profile around each protein, which, in turn, could induce conformational changes in the proteins. Furthermore, if an overshooting/undershooting effect exists, one should be careful in the interpretation of data obtained from spectroscopic measurements of the lipid order parameter, S. If the number of overshooting (undershooting) lipids around proteins is sufficiently high (thus to affect the system in a experimentally detectable manner), the calculation of the lipid bilayer hydrophobic thickness derived from spectroscopy measurements of S could underestimate (overestimate) the value of the thickness.

We would like to add that, in the present work, we have focused on a model for DMPC bilayers, and on embedded proteins that are isotropically hydrophobic. Nevertheless, our results may be qualitatively applied to other lipid bilayers as well. In fact, a possible way of varying the hydrophobic mismatch is to study the same model proteins in bilayers with different acyl chains lengths, i.e., longer or shorter than those of DMPC. Also, the model could be used to investigate lipid bilayers with embedded amphiphatic membrane peptides, such as the antimicrobial peptide of fungal origin, alamethicin (He et al., 1995; Duclohier and Wróblewski, 2001), or the peptide phospholamban, forming a cardiac ion channel (Arkin et al., 1994). These peptides attach first to the lipid-water interface through their hydrophobic side, and then insert into the membrane once their interfacial concentration reaches a critical value (Shai, 1995; Bechinger, 1999). The aggregation process results in the formation of membrane channels. The size of these channels may depend, among other factors, on the hydrophobic mismatch interaction (He et al., 1995; Sperotto, 1997). In the future, we plan to investigate the insertion and aggregation process of model amphiphatic peptides (i.e., the lifetime and stability of the aggregates), and its dependence on peptide concentration and mismatch.

We want to conclude that a number of biomembrane processes involve extensive and cooperative molecular rearrangements in the membrane plane, via, among others, diffusion of molecules. Such rearrangements may occur over a timescale that might be outside the range of investigation of more traditional simulation techniques, such as MD on all-atom models. The use of the DPD-simulation CG-model approach can allow us to study larger system sizes, and for longer times, than those permitted by MD simulations on all-atom models. Therefore, by the DPD-simulation CG-model approach, one can access properties related to the cooperative behavior of a bilayer system.

M.M.S. is grateful to Marcus A. Hemminga (Wageningen University, The Netherlands), Morten Ø. Jensen and John H. Ipsen (both at The University of Southern Denmark, Denmark), and to J. Antoinette Killian (Utrecht University, The Netherlands), for numerous stimulating discussions. M.M.S. thanks the Center for Biological Sequence Analysis (in particular, Kristoffer Rapacki) both at the Biochemistry and Nutrition Group (in particular, Ib Søndergaard), and the Biocentrum-DTU (The Technical University of Denmark, Denmark), for hospitality and support.

This work is part of the research program of the Stichting voor Fundamenteel Onderzoek der Materie, which is financially supported by the Nederlandse Organisatie voor Wetenschappelijk Onderzoek.

REFERENCES

Arkin, I. T., P. D. Adam, K. R. MacKenzie, M. L. Lemmon, A. T. Brünger, and D. Engelman. 1994. Structural organization of the pentameric transmembrane α-helices of phospholamban, a cardiac ion channel. *EMBO J.* 13:4757–4764.

Bechinger, B. 1999. The structure, dynamics and orientation of antimicrobial peptides in membranes by multidimensional solid-state NMR spectroscopy. *Biochim. Biophys. Acta.* 1462:157–183.

Bechinger, B. 1997. Structure and dynamics of the M13 coat signal sequence in membranes by multidimensional high-resolution and solid-state NMR spectroscopy. *Proteins Struct. Funct. Genet.* 27:481–492.

Belohorcová, K., J. H. Davis, T. B. Woolf, and B. Roux. 1997. Structure and dynamics of an amphiphilic peptide in a bilayer: a molecular dynamics study. *Biophys. J.* 73:3039–3055.

Belohorcová, K., J. Qian, and J. H. Davis. 2000. Molecular dynamics and ^{2}H-NMR study of the influence of an amphiphilic peptide on membrane order and dynamics. *Biophys. J.* 79:3201–3016.

Binder, W. H., V. Barragan, and F. M. Menger. 2003. Domains and rafts in lipid membranes. *Angew. Chem. Int. Ed.* 42:5802–5827.

Bohinc, K., V. Kralj-Iglič, and S. May. 2003. Interaction between two cylindrical inclusions in a symmetric lipid-bilayer. *J. Chem. Phys.* 119: 7435–7444.

Brasseur, R. 2000. Tilted peptides: a motif for membrane destabilization (hypothesis). *Mol. Membr. Biol.* 17:31–40.

Bretscher, M. S., and S. Munro. 1993. Cholesterol and the Golgi apparatus. *Science.* 261:1280–1281.

Bryl, K., and K. Yoshihara. 2001. The role of retinal in the long-range protein-lipid interactions in bacteriorhodopsin-phosphatidylcholine vesicles. *Eur. Biophys. J.* 29:628–640.

Canningham, B. A., A.-D. Brown, D. H. Wolfe, D. P. Williams, and A. Brain. 1998. Ripple phase formation in phosphatidylcholine: effect of acyl chain relative length, position and unsaturation. *Phys. Rev. E.* 58: 3662–3672.

Chiu, S.-W., M. Clark, V. Balaji, S. Subramaniam, H. L. Scott, and E. Jakobsson. 1995. Incorporation of surface tension into molecular dynamics simulation of an interface: a fluid phase lipid bilayer membrane. *Biophys. J.* 69:1230–1245.

Chiu, S.-W., S. Subramaniam, and E. Jakobsson. 1999. Simulation study of a gramicidin/lipid bilayer system in excess water and lipid. I. Structure of the molecular complex. *Biophys. J.* 76:1929–1938.

Dan, N., and S. A. Safran. 1998. Effect of lipid characteristics on the structure of transmembrane proteins. *Biophys. J.* 75:1410–1414.

de Planque, M. R. R., E. Goormaghtigh, D. V. Greathouse, R. E. Koeppe, II, J. A. W. Kruijtzer, R. M. J. Liskamp, B. de Kruijff, and J. A. Killian. 2001. Sensitivity of single membrane-spanning α-helical peptides to hydrophobic mismatch with a lipid bilayer: effects on backbone structure, orientation, and extent of membrane incorporation. *Biochemistry*. 40:5000–5010.

de Planque, M. R. R., and J. A. Killian. 2003. Protein-lipid interactions studied with designed transmembrane peptides: role of hydrophobic matching and interfacial anchoring. *Mol. Membr. Biol.* 20:271–284.

Deisenhofer, J., O. Epp, K. Miki, R. Huber, and H. Michael. 1985. Structure of the protein subunits in the photosynthetic reaction center of *Rhodopseudomonas viridis* at 3 Å resolution. *Nature*. 318:618–624.

Duclohier, H., and H. Wróblewski. 2001. Voltage-dependent pore formation and antimicrobial activity by alamethicin and analogues. *J. Membr. Biol.* 184:1–12.

Dumas, F., M. M. Sperotto, M. C. Lebrum, J.-F. Tocanne, and O. G. Mouritsen. 1997. Molecular sorting of lipids by bacteriorhodopsin in dilauroylphosphatidylcholine/distearoylphosphatidylcholine lipid bilayers. *Biophys. J.* 73:1940–1953.

Dumas, F., M. C. Lebrum, and J.-F. Tocanne. 1999. Is the protein/lipid hydrophobic matching principle relevant to membrane organization and functions? *FEBS Lett.* 458:271–277.

Duque, D., X. Li, K. Katsov, and M. Schick. 2002. Molecular theory of hydrophobic mismatch between lipids and peptides. *J. Chem. Phys.* 116:10478–10484.

Epand, R. M. 1998. Lipid polymorphism and lipid-protein interactions. *Biochim. Biophys. Acta*. 1376:353–368.

Español, P., and P. Warren. 1995. Statistical mechanics of dissipative particle dynamics. *Europhys. Lett.* 30:191–196.

Fahsel, S., E.-M. Pospiech, M. Zein, T. L. Hazlet, E. Gratton, and R. Winter. 2002. Modulation of concentration fluctuations in phase-separated lipid membranes by polypeptide insertion. *Biophys. J.* 83: 334–344.

Fantini, J., N. Garmy, R. Mahfoud, and N. Yahi. 2002. Lipid rafts: structure, function and role in HIV, Alzheimer's and prion diseases. *In* Expert Reviews in Molecular Medicine. Cambridge University Press, Cambridge, UK. 1–22.

Fattal, D. R., and A. Ben-Shaul. 1993. A molecular model for lipid-protein interactions in membranes: the role of hydrophobic mismatch. *Biophys. J.* 65:1795–1809.

Feller, S. E., and R. W. Pastor. 1996. On simulating lipid bilayers with an applied surface tension: periodic boundary conditions and undulations. *Biophys. J.* 71:1350–1355.

Feller, S. E., and R. W. Pastor. 1999. Constant surface tension simulations of lipid bilayers: the sensitivity of surface areas and compressibilities. *J. Chem. Phys.* 111:1281–1287.

Fernandes, F., L. M. S. Loura, M. Prieto, R. Koehorst, R. B. Spruijt, and M. A. Hemminga. 2003. Dependence of M13 major coat protein oligomerization and lateral segregation on bilayer composition. *Biophys. J.* 85:2430–2441.

Foster, D. L., M. Boublik, and H. R. Kaback. 1983. Structure of the Lac carrier protein of *Escherichia coli*. *J. Biol. Chem.* 258:31–34.

Fu, D., A. Libson, L. J. W. Miercke, C. Weitzman, P. Nollert, J. Krucinski, and R. M. Stround. 2000. Structure of a glycerol-conducting channel and the basis for its selectivity. *Science*. 290:481–486.

Gil, T., and J. H. Ipsen. 1997. Capillary condensation between disks in two dimensions. *Phys. Rev. E*. 55:1713–1721.

Gil, T., J. H. Ipsen, O. G. Mouritsen, M. C. Sabra, M. M. Sperotto, and M. J. Zuckermann. 1998. Theoretical analysis of protein organization in lipid membranes. *Biochim. Biophys. Acta*. 1376:245–266.

Glaubitz, C., G. Grobner, and A. Watts. 2000. Structural and orientational information of the membrane embedded M13 coat protein by ^{13}C-MAS NMR spectroscopy. *Biochim. Biophys. Acta*. 1463:151–161.

Goetz, R., and R. Lipowsky. 1998. Computer simulations of bilayer membranes: self-assembly and interfacial tension. *J. Chem. Phys.* 108: 7397–7409.

Goetz, R., G. Gompper, and R. Lipowsky. 1998. Mobility and elasticity of self-assembled membranes. *Phys. Rev. Lett.* 82:221–224.

Groot, R. D. 2000. Mesoscopic simulation of polymer-surfactant aggregation. *Langmuir*. 16:7493–7502.

Groot, R. D., and K. L. Rabone. 2001. Mesoscopic simulation of cell membrane damage, morphology change and rupture by nonionic surfactant. *Biophys. J.* 81:725–736.

Groot, R. D., and P. Warren. 1997. Dissipative particle dynamics: bringing the gap between atomistic and mesoscopic simulation. *J. Chem. Phys.* 107:4423–4435.

Harroun, T. A., W. T. Heller, T. M. Weiss, L. Yang, and H. W. Huang. 1999. Experimental evidence for hydrophobic matching and membrane-mediated interactions in lipid bilayers containing gramicidin. *Biophys. J.* 76:937–945.

Harzer, U., and B. Bechinger. 2000. Alignment of lysine-anchored membrane peptides under conditions of hydrophobic mismatch: a CD, ^{15}N and ^{31}P solid-state NMR spectroscopy investigation. *Biochemistry*. 39:13106–13114.

Henderson, R., and P. N. T. Unwin. 1975. Three-dimensional model of purple membrane obtained by electron microscopy. *Nature*. 257:28–32.

He, K., S. J. Ludke, H. W. Huang, and D. Worcester. 1995. Antimicrobial peptide pores in membranes detected by neutron in-plane scattering. *Biochemistry*. 34:15614–15618.

Hesketh, T. R., G. A. Smith, M. D. Houslay, K. A. McGill, N. J. M. Birdsall, J. C. Metcalfe, and G. B. Warren. 1976. Annular lipids determine the ATPase activity of a calcium transport protein complexed with dipalmitoyl-lecithin. *Biochemistry*. 15:4145–4151.

Hoogerbrugge, P. J., and J. M. V. A. Koelman. 1992. Simulating microscopic hydrodynamics phenomena with dissipative particle dynamics. *Europhys. Lett.* 19:155–160.

In't Veld, G., A. J. M. Driessen, J. A. F. Op den Kamp, and W. N. Konings. 1991. Hydrophobic membrane thickness and lipid-protein interactions of the leucine transport system of *Lactococcus lactis*. *Biochim. Biophys. Acta*. 1065:203–212.

Iwata, S., C. Ostermeier, B. Ludwig, and H. Michael. 1995. Structure at 2.8 Å resolution of cytochrome-c oxidase from *Paracoccus denitrificans*. *Nature*. 376:660–669.

Jähnig, F. 1996. What is the surface tension of a lipid membrane? *Biophys. J.* 71:1348–1349.

Jensen, M. Ø., and O. G. Mouritsen. 2004. Lipids do influence protein function—the hydrophobic matching hypothesis revised. *Biochim. Biophys. Acta*. 1666:205–226.

Jensen, M. Ø., E. Tajkhorshid, and K. Schulten. 2001. The mechanism of glycerol conduction in aquaglyceroporins. *Structure*. 9:1083–1093.

Jensen, M.Ø., S. Park, E. Tajkhorshid, and K. Schulten. 2002. Energetics of glycerol conduction through aquaglyceroporin GlpF. *Proc. Natl. Acad. Sci. USA*. 99:6731–6736.

Johansson, A., G. A. Smith, and J. Metcalfe. 1981. The effect of bilayer thickness on the activity of $(Na^+$-$K^+)$-ATPase. *Biochim. Biophys. Acta*. 641:416–421.

Jost, P. C., and O. Hayes Griffith. 1980. The lipid-protein interface in biological membranes. *Ann. NY Acad. Sci. USA*. 348:391–405.

Jost, P. C., O. Hayes Griffith, R. A. Capaldi, and G. Vanderkooi. 1973. Evidence for boundary lipids in membranes. *Proc. Natl. Acad. Sci. USA*. 70:480–484.

Jury, S., P. Bladon, M. Cates, S. Krishna, M. Hagen, N. Ruddock, and P. Warren. 1999. Simulation of amphiphilic mesophases using dissipative particle dynamics. *Phys. Chem. Chem. Phys.* 1:2051–2056.

Killian, J. A. 1992. Gramicidin and gramicidin-lipid interactions. *Biochim. Biophys. Acta*. 1113:391–425.

Killian, J. A. 1998. Hydrophobic mismatch between proteins and lipids in membranes. *Biochim. Biophys. Acta*. 1376:401–416.

Koehorst, R. B. M., R. B. Spruijt, F. J. Vergeldt, and M. A. Hemminga. 2004. Lipid bilayer topology of the transmembrane α-helix of M13 major

coat protein and bilayer polarity profile by site-directed fluorescence spectroscopy. *Biophys. J.* 87:1445–1455.

Kol, M. A., A. van Delen, A. I. P. M. de Kroon, and B. de Kruijff. 2003. Translocation of phospholipids is facilitated by a subset of membrane-spanning proteins of the bacterial cytoplasmic membrane. *J. Biol. Chem.* 278:24586–24593.

Koynova, R., and M. Caffrey. 1998. Phases and phase transitions of the phosphatidylcholines. *Biochim. Biophys. Acta.* 1376:91–145.

Kranenburg, M., M. Venturoli, and B. Smit. 2003a. Molecular simulations of mesoscopic bilayer phases. *Phys. Rev. E.* 67:060901.

Kranenburg, M., M. Venturoli, and B. Smit. 2003b. Phase behavior and induced interdigitation in bilayer studied with dissipative particle dynamics. *J. Phys. Chem. B.* 107:11491–11501.

Kranenburg, M., and B. Smit. 2004. Simulating the effects of alcohol on the structure of a membrane. *FEBS Lett.* 568:15–18.

Kranenburg, M., J. P. Nicolas, and B. Smit. 2004a. Comparison of mesoscopic phospholipid-water models. *Phys. Chem. Chem. Phys.* 6: 4142–4151.

Kranenburg, M., M. Vlaar, and B. Smit. 2004b. Simulating induced interdigitation in membranes. *Biophys. J.* 87:1596–1605.

Kranenburg, M., C. Laforge, and B. Smit. 2004c. Mesoscopic simulations of phase transitions in lipid bilayers. *Phys. Chem. Chem. Phys.* 6:4531–4534.

König, S., and E. Sackmann. 1996. Molecular and collective dynamics of lipid bilayers. *Curr. Opin. Colloid Interface Sci.* 1:78–82.

Lee, A. G. 1998. How lipids interact with an intrinsic membrane protein: the case of the calcium pump. *Biochim. Biophys. Acta.* 1376:381–390.

Lee, A. G. 2003. Lipid-protein interactions in biological membranes: a structural perspective. *Biochim. Biophys. Acta.* 1612:1–40.

Lehtonen, J. Y. A., and P. K. J. Kinnunen. 1997. Evidence for phospholipid microdomain formation in liquid crystalline liposomes reconstituted with *Escherichia coli* lactose permease. *Biophys. J.* 72:1247–1257.

Lins, L., B. Charloteaux, A. Thomas, and R. Brasseur. 2001. Computational study of lipid-destabilizing protein fragments: towards a comprehensive view of tilted peptides. *Proteins Struct. Funct. Genet.* 44: 435–447.

Liu, F., R. N. A. H. Lewis, R. S. Hodges, and R. N. McElhaney. 2002. Effect of variations in the structures of a polyleucine-based α-helical transmembrane peptide on its interaction with phosphatidylcholine bilayers. *Biochemistry.* 41:9197–9207.

MacKenzie, K. R., J. H. Prestegard, and D. M. Engelmann. 1997. A transmembrane helix dimer: structure and implications. *Science.* 276: 131–133.

Mall, S., R. Broadbridge, R. P. Sharma, J. M. East, and A. G. Lee. 2001. Self-association of model transmembrane helix is modulated by lipid structure. *Biochemistry.* 40:12379–12386.

Marrink, S.-J., E. Lindahl, O. Edholm, and A. E. Mark. 2001. Simulation of the spontaneous aggregation of phospholipids into bilayers. *J. Am. Chem. Soc.* 123:8638–8639.

Marrink, S. J., and A. E. Mark. 2001. Effect of undulations on surface tension in simulated bilayers. *J. Phys. Chem. B.* 105:6122–6127.

May, S. 2000. Theories on structural perturbations of lipid bilayers. *Curr. Opin. Colloid Interface Sci.* 5:244–249.

McIntosh, T. J., A. Vidal, and S. A. Simon. 2003. Sorting of lipids and transmembrane peptides between detergent-soluble bilayers and detergent-resistant rafts. *Biophys. J.* 85:1656–1666.

Montecucco, C., G. A. Smith, F. Dabbeni-Sala, A. Johansson, Y. M. Galante, and R. Bisson. 1982. Bilayer thickness and enzymatic activity in the mitochondrial cytochrome-C oxidase and ATPase complex. *FEBS Lett.* 144:145–148.

Morein, S., J. A. Killian, and M. M. Sperotto. 2002. Characterization of the thermotropic behavior and lateral organization of lipid-peptide mixtures by a combined experimental and theoretical approach: effects of hydrophobic mismatch and role of flanking residues. *Biophys. J.* 82: 1405–1417.

Mouritsen, O. G. M. 1998. Self-assembly and organization of lipid-protein membranes. *Curr. Opin. Colloid Interface Sci.* 3:78–87.

Mouritsen, O. G., and M. Blom. 1984. Mattress model of lipid-protein interactions in membranes. *Biophys. J.* 46:141–153.

Mouritsen, O. G., and M. M. Sperotto. 1993. Thermodynamics of lipid-protein interactions in lipid membranes. *In* Thermodynamics of Membrane Receptors and Channels. M. Jackson, editor. CRC Press, Boca Raton, FL. 127–181.

Mouritsen, O. G., M. M. Sperotto, J. Risbo, Z. Zhang, and M. J. Zuckermann. 1996. Computational approach to lipid-protein interactions in membranes. *Adv. Comp. Biol.* 2:15–64.

Munro, S. 1995. An investigation of the role of transmembrane domain in Golgi protein retention. *EMBO J.* 14:4695–4704.

Munro, S. 1998. Localization of proteins to the Golgi apparatus. *Trends Cell Biol.* 8:11–15.

Nevzorov, A. A., M. F. Mesleh, and S. J. Opella. 2004. Structure determination of aligned samples of membrane proteins by NMR spectroscopy. *Magn. Reson. Chem.* 42:162–171.

Nielsen, C., M. Goulian, and O. S. Andersen. 1998. Energetics of inclusion-induced bilayer deformations. *Biophys. J.* 74:1966–1983.

Pelham, H. R. B., and S. Munro. 1993. Sorting of membrane-proteins in the secretory pathway. *Cell.* 75:603–605.

Petrache, H. I., S. W. Dodd, and M. F. Brown. 2000a. Area per lipid and acyl length distributions in fluid phosphatidylcholines determined by ^{2}H NMR spectroscopy. *Biophys. J.* 79:3172–3192.

Petrache, H. I., A. Grossfield, K. R. MacKenzie, D. M. Engelman, and T. Woolf. 2000b. Modulation of glycophorin A transmembrane helix interactions by lipid bilayers: molecular dynamics calculations. *J. Mol. Biol.* 302:727–746.

Petrache, H. I., D. M. Zuckerman, J. N. Sachs, J. A. Killian, R. E. Koeppe II, and T. Woolf. 2002. Hydrophobic matching by molecular dynamics simulations. *Langmuir.* 18:1340–1351.

Piknová, B., E. Pérochon, and J.-F. Tocanne. 1993. Hydrophobic mismatch and long-range protein/lipid interactions in bacteriorhodopsin/phosphatidylcholine vesicles. *Eur. J. Biochem.* 218:385–396.

Rehorek, M., N. A. Dencher, and M. P. Heyn. 1985. Long-range lipid-protein interactions. Evidence from time-resolved fluorescence depolarization and energy-transfer experiments with bacteriorhodopsin-dimyristoylphosphatidylcholine vesicles. *Biochemistry.* 24:5980–5988.

Ridder, A. N. J. A., E. R. J. Spelbrink, J. A. A. Demmers, D. T. S. Rijkers, R. M. J. Liskamp, J. Brunner, A. J. R. Heck, B. De Kruijff, and J. A. Killian. 2004. Photo-crosslinking analysis of preferential interactions between a transmembrane peptide and matching lipids. *Biochemistry.* 43:4482–4489.

Ridder, A. N. J. A., W. Van De Hoef, J. Stam, A. Kuhn, B. De Kruijff, and J. A. Killian. 2002. Importance of hydrophobic matching for spontaneous insertion of a single-spanning membrane protein. *Biochemistry.* 41: 4946–4952.

Sackmann, E. 1984. Physical basis of trigger processes and membrane structure. *In* Biological Membranes, Vol. 5. D. Chapman, editor. Academic Press, London, UK. 105–143.

Sackmann, E. 1995. Biological membranes architecture and function. *In* Structure and Dynamics of membranes. Lipowsky, R. and Sackmann, E., editors. Elsevier, Amsterdam. 1–65.

Shai, Y. 1995. Molecular recognition between membrane-spanning polypeptides. *Trends Biochem. Sci.* 20:460–464.

Sharpe, S., K. R. Barber, C. W. M. Grant, D. Goodyear, and M. R. Morrow. 2002. Organization of model helical peptides in lipid bilayers: insight into the behavior of single-span protein transmembrane domains. *Biophys. J.* 83:345–358.

Shen, L., D. Bassolino, and T. Stouch. 1997. Transmembrane helix structure, dynamics, and interactions: multi-nanoseconds molecular dynamics simulations. *Biophys. J.* 73:3–20.

Shelley, J. C., M. Y. Shelley, R. C. Reeder, S. Badyopadhyay, and M. L. Klein. 2001a. A coarse-grain model for phospholipid simulations. *J. Phys. Chem. B.* 105:4464–4470.

Shelley, J. C., M. Y. Shelley, R. C. Reeder, S. Badyopadhyay, P. B. Moore, and M. L. Klein. 2001b. Simulations of phospholipids using a coarse-grain model. *J. Phys. Chem. B.* 105:9785–9792.

Simons, K., and E. Ikonen. 1997. Functional rafts in cell membranes. *Nature*. 387:569–572.

Sintes, T., and A. Baumgärtner. 1998. Protein attraction in membranes induced by lipid fluctuations. *Biophys. J.* 73:2251–2259.

Sperotto, M. M. 1997. A theoretical model for the association of amphiphilic transmembrane peptides in lipid bilayers. *Eur. Biophys. J.* 26:405–416.

Sperotto, M. M., and O. G. Mouritsen. 1991. Monte Carlo simulation studies of lipid order parameter profiles near integral membrane proteins. *Biophys. J.* 59:261–270.

Stopar, D., R. B. Spruijt, C. J. A. M. Wolfs, and M. A. Hemminga. 2003. Protein-lipid interactions of bacteriophage M13 major coat protein. *Biochim. Biophys. Acta.* 1611:5–15.

Strandberg, E., S. Özdirekcan, D. T. S. Rijkers, P. C. A. van der Wel, R. E. Koeppe II, R. M. J. Liskamp, and J. A. Killian. 2004. Tilt angles of transmembrane model peptides in oriented and non-oriented lipid bilayers as determined by ^{2}H solid-state NMR. *Biophys. J.* 86:3709–3721.

Thomson, T. E., M. B. Sankaram, R. B. Biltonen, D. Marsh, and W. L. C. Vaz. 1995. Effect of domain structure on in-plane reactions and interactions. *Mol. Membr. Biol.* 12:157–162.

Tocanne, J.-F. 1992. Detection of lipid domains in biological membranes. *Comm. Mol. Cell. Biophys.* 8:53–72.

Tocanne, J.-F., L. Cézanne, A. Lopaz, B. Piknová, V. Schram, J. F. Turnier, and M. Welby. 1994. Lipid domains and lipid/protein interactions in biological membranes. *Chem. Phys. Lipids.* 73:139–159.

Tristram-Nagle, S., Y. Liu, J. Legleiter, and J. F. Nagle. 2002. Structure of gel phase DMPC determined by x-ray diffraction. *Biophys. J.* 83:3324–3335.

van der Wel, P. C. A., E. Strandberg, J. A. Killian, and R. E. Koeppe II. 2002. Geometry and intrinsic tilt of a tryptophan-anchored transmembrane α-helix determined by ^{2}H NMR. *Biophys. J.* 83:1479–1488.

Venturoli, M., and B. Smit. 1999. Simulating the self-assembly of model membranes. *Phys. Chem. Comm.* 10:1–5.

von Heijne, G., and M. Manoil. 1990. Membrane proteins: from sequence to structure. *Protein Eng.* 4:109–112.

Warren, P. B. 1998. Dissipative particle dynamics. *Curr. Opin. Colloid Interface Sci.* 3:620–624.

Weiss, T. M., P. C. A. van der Wel, J. A. Killian, R. E. Koeppe II, and H. W. Huang. 2003. Hydrophobic mismatch between helices and lipid bilayers. *Biophys. J.* 84:379–385.

Zhang, Y., S. E. Feller, B. R. Brooks, and R. W. Pastor. 1995. Computer simulation of liquid/liquid interfaces. I. Theory and application to octane/water. *J. Chem. Phys.* 103:10252–10266.